Universidade de Aveiro
2020

Ana Isabel Oliveira Campos

Identificação de cinases reguladoras da subunidade beta do complexo FoF1 ATP sintase

Identification of regulatory kinases of the FoF1 ATP synthase beta subunit

Universidade de Aveiro
2020

Ana Isabel Oliveira Campos

Identificação de cinases reguladoras da subunidade beta do complexo FoF1 ATP sintase

Identification of regulatory kinases of the FoF1 ATP synthase beta subunit

Dissertação apresentada à Universidade de Aveiro para cumprimento dos requisitos necessários à obtenção do grau de Mestre em Biologia Molecular e Celular, realizada sob a orientação científica da Doutora Clara Isabel Ferreira Pereira, Investigadora Auxiliar no Instituto de Investigação e Inovação em Saúde (i3S) da Universidade do Porto e coorientação da Doutora Maria Paula Polónia Gonçalves, Professora Associada do Departamento de Biologia da Universidade de Aveiro.

This work was funded by National Funds through FCT—Fundação para a Ciência e a Tecnologia, I.P., under the projects IF/00889/2015/CP1303/CT0004 and UIDB/04293/2020

“Don't waste your time on jealousy
Sometimes you're ahead, sometimes you're behind
The race is long and, in the end, it's only with yourself.”

- Baz Luhrmann

o júri

Presidente	Professor Doutor Artur Jorge da Costa Peixoto Alves Professor Auxiliar c/ Agregação, Universidade de Aveiro
Vogal - Arguente	Doutora Maria Margarida de Sá Duarte Investigadora Auxiliar, IBMC/I3S, Universidade do Porto
Vogal - Orientadora	Doutora Clara Isabel Ferreira Pereira Investigadora Auxiliar, IBMC/I3S, Universidade do Porto

Agradecimentos

Em primeiro lugar, gostaria de agradecer à minha orientadora Dra. Clara Pereira, por me ter proporcionado esta oportunidade, pela paciência, compreensão e amizade. Agradeço ainda toda a ajuda e partilha de conhecimentos. O que aprendi ao longo deste percurso, vai sem dúvida tornar-me numa melhor profissional.

Em segundo lugar, gostaria de agradecer ao Professor Vitor Costa e aos restantes membros do grupo *Yeast Signaling Networks* por me terem recebido de braços abertos e por me terem feito sentir em casa. Foi um prazer aprender ao lado de pessoas tão extraordinárias, que sempre se disponibilizaram para me ajudar. Um especial obrigado à Cláudia, por todas as dicas preciosas que tanto me facilitaram a vida.

Em terceiro lugar, gostaria de agradecer à Professora Paula Gonçalves pela disponibilidade para coorientar esta dissertação e pelas sugestões na elaboração deste manuscrito.

Ao grupo *Phenotypic Evolution*, agradeço a vossa simpatia, amizade e constante boa disposição, especialmente importante neste ano tão atípico.

À Raquel, Párástu e Quaresma, agradeço por ouvirem todos os meus desabafos, por todos os "*there there*", por todas as sessões de brainstorming e por me fazerem ver que há sempre uma solução.

À Diana, Beatriz, Daniela e Alves obrigada pela amizade interminável, sem vocês esta jornada não faria sentido.

Ao Gonçalo, por partilhares a tua vida comigo, por apoiares todas as minhas decisões e por acreditares em mim a dobrar nos dias em que o cansaço fez com que eu deixasse de acreditar.

Ao meu irmão e à Juliana, por todo o apoio e pelos conselhos.

Por último, agradeço aos meus pais. Obrigada pelo apoio incansável, pelo amor e carinho incondicional. Sem os vossos esforços e sacrifícios nada disto seria possível. Sou-vos eternamente grata.

Palavras-chave *S. cerevisiae*, mitocôndria, subunidade β ATP sintase, fosforilação, fosforegulação, Phos-Tag™, cinases reguladoras, Cdc5.

Resumo

Em eucariotas superiores, cerca de 90% do ATP celular é produzido pela ATP sintase, um complexo enzimático mitocondrial. Várias modificações pós-tradução, especialmente fosforilação, foram descritas em todas as subunidades da ATP sintase, tanto em condições fisiológicas normais como patológicas. No entanto, o impacto destas modificações na regulação da ATP sintase ou as vias de sinalização envolvidas precisam ainda de elucidação.

Recentemente, dois locais de fosforilação foram identificados na subunidade β, catalítica, da ATP sintase (Atp2) em *S. cerevisiae*, Treonina (Thr) 124 e Thr317. A fosforilação destes resíduos promove a estabilização de Atp2p, e o aumento da atividade da ATP sintase e da respiração mitocondrial. Porém as cinases envolvidas na fosforilação destes resíduos, conservados entre espécies, são ainda desconhecidas. Usando *S. cerevisiae* como modelo, o objetivo deste estudo consistiu em identificar cinase(s) envolvida(s) na fosforegulação da subunidade β da ATP sintase.

A utilização de ferramentas bioinformáticas de algoritmo preditivo de locais de fosforilação, permitiu a seleção de 4 cinases como potenciais reguladores de Atp2p: Cdc5, Ipl1, Hrr25 e Pkc1. Foi ainda avaliada a Cdc28, após observação prévia de interação genética com Atp2p. A expressão das cinases foi manipulada de forma a avaliar possíveis efeitos na fosforilação e nos níveis de Atp2p. O método Zn^{2+}Phos-Tag™ SDS-PAGE foi otimizado e utilizado para deteção da fosforilação de Atp2p. A sobrexpressão de Cdc5, Ipl1 e Pkc1 levou a um aumento da fosforilação de Atp2p. A sobrexpressão de Ipl1 aumentou também os níveis de Atp2p, consistentes com aumento de fosforilação, enquanto que um aumento pouco significativo foi observado para Cdc5. O papel da Cdc5 na função mitocondrial foi estudado, sendo que a sua sobrexpressão causou um aumento significativo da respiração mitocondrial e a repressão de Cdc5 inibiu o crescimento em meio respiratório, sugerindo que a Cdc5 possa ter um efeito regulador importante na função mitocondrial. Mais estudos são necessários para determinar se Cdc5 é um fosforegulador direto de Atp2p.

A identificação de cinases reguladoras de Atp2p contribuirá para o conhecimento das vias de sinalização que regulam a função da ATP sintase. Visto que várias patologias estão associadas à disfunção deste complexo essencial, a identificação das suas cinases reguladoras pode nomear, a longo prazo, novos alvos terapêuticos.

Keywords *S. cerevisiae*, mitochondria, ATP synthase β subunit, phosphorylation, phosphoregulation, Phos-Tag™, regulatory kinases, Cdc5.

Abstract

In higher eukaryotes, approximately 90% of cellular ATP is produced by ATP synthase, a mitochondrial enzymatic complex. Numerous post-translational modifications, particularly phosphorylation, were reported for all ATP synthase subunits, both in physiological and pathological states. Still, the impact of these modifications for ATP synthase regulation or the signaling pathways involved remains ill-defined.

Previously, two phosphorylation sites were identified in the catalytic β subunit of the FoF1 ATP synthase (Atp2) of *S. cerevisiae*, Threonine 124 (Thr) and Thr317. Phosphorylation of these residues resulted in Atp2p stabilization, increased ATP synthase activity and mitochondrial respiration. Yet, the kinases involved in the phosphorylation of these residues, conserved across species, are unknown. Using *S. cerevisiae* as a model, the aim of this study was thus to identify the kinase(s) involved in the phosphoregulation of the ATP synthase β subunit.

Using bioinformatic motif prediction, four kinases were selected as potential Atp2 regulators: Cdc5, Ipl1, Hrr25 and Pkc1. Cdc28 was also evaluated since a genetic interaction with Atp2 was previously observed. Kinase expression was manipulated to evaluate possible effects in Atp2p phosphorylation and Atp2p levels. Zn^{2+}Phos-Tag™ SDS-PAGE was optimized and used to detect Atp2p phosphorylation. The overexpression of Pkc1, Ipl1 and Cdc5 resulted in increased Atp2 phosphorylation. Overexpressing Ipl1 also caused an increase in Atp2p levels, consistent with increased phosphorylation, while a minor increase was observed for Cdc5. The role of Cdc5 on mitochondrial function was further evaluated. Overexpression of Cdc5 resulted in a significant increase in mitochondrial respiration and repressing Cdc5 prevented growth in respiratory media, indicating that Cdc5 plays an important, previously unsuspected role in mitochondrial function.

Though overall evidence supports a role for Cdc5 in Atp2 regulation, further studies are required to confirm that Cdc5 is, in fact, a direct phosphoregulator of Atp2. Identification of Atp2p regulatory kinases will improve our understanding of the signalling pathways regulating ATP synthase function. Since many pathologies are associated with dysfunction of this vital complex, identification of its regulatory kinases can provide, in the long run, new therapeutic targets.

Index

List of Tables

Figure List

Supplementary Figure List

Abbreviations

2DE	Two-dimensional Gel Electrophoresis
3'UTR	3′-Untranslated Region
^{32}P	Radioactive Phosphorus-32
ADP	Adenosine Diphosphate
ATP	Adenosine Triphosphate
ATPsyn-β	β subunit of ATP Synthase (mammals)
Da	Daltons
G3BP1	Ras-GAP SH3 binding protein 1
Gal	Galactose
Glc	Glucose
IF1	ATPase Inhibitory Factor 1
IMM	Inner Mitochondrial Membrane

IP	Isoelectric Point
mPTP	Mitochondrial Permeability Transition Pore
MS	Mass Spectrometry
mtDNA	Mitochondrial DNA
nDNA	Nuclear DNA
OCR	Oxygen Consumption Rate
OD_{600}	Optical Density at 600nm
OMM	Outer Mitochondrial Membrane
OXPHOS	Oxidative Phosphorylation
PCR	Polymerase Chain Reaction
pDNA	Plasmid DNA
p*GAL1*	*GAL1* promoter
PI	Inorganic Phosphate
PKCα	Protein kinase C α
PKCδ	Protein kinase C δ
p*MET25*	*MET25* promoter
PTM	Post-translational Modifications
RPM	Revolutions per Minute
Ser	Serine
TBS	Tris-buffered Saline
TCA	Trichloroacetic Acid
Thr	Threonine
Ts	Temperature-sensitive
TTBS	TBS with 0.05% (vol/vol) Tween-20
Tyr	Tyrosine
Wt	Wild type
YPC	Yeast Peptone Combo (1.5%Gal +0.5%Glc)
YPD	Yeast Peptone Dextrose
YPGal	Yeast Peptone Galactose
YPGly	Yeast Peptone Glycerol

1. Introduction

1. Mitochondria

The very existence of living organisms depends on energy production. The anaerobes, the first organisms to populate the Earth, relied on processes such as fermentation and glycolysis to fulfill their energy needs. However, these processes are rather inefficient and resulted in the excretion of high energy products that simply could not be further metabolized by anaerobic organisms (Karp, Iwasa and Marshall, 2015). The emergence of oxygen-releasing cyanobacteria caused a shift in the composition of the planet's atmosphere and the resulting surplus of oxygen drove organisms to evolve into more complex lifeforms, which ultimately gave rise to present day oxygen-dependent prokaryotes and eukaryotes. These organisms satisfy their energy requirements due to an adenosine triphosphate (ATP)-producing mechanism based on the transport of electrons along membranes, allowing the extraction of energy from various food sources during cell respiration (Alberts *et al.*, 2013; Karp, Iwasa and Marshall, 2015).

In eukaryotic cells, the majority of ATP is produced via oxidative phosphorylation (OXPHOS) in the mitochondrion, a specialized organelle present in nearly all eukaryotic cells (Alberts *et al.*, 2013; Filograna *et al.*, 2020). Mitochondria are highly adaptable organelles, capable of adjusting their number, shape and location suiting the metabolic requirements of the cell and assuming different structures according to the cell type (Detmer and Chan, 2007; Westermann, 2012). These highly dynamic organelles undergo constant structural transitions, having a broad spectrum of morphologies that range from a bean-shaped organelle to an interconnected and highly branched tubular network (Karp, Iwasa and Marshall, 2015).

Mitochondrial morphology is a result of two opposing processes, fusion and fission, according to the energy requirements of the cell (Kanfer and Kornmann, 2016). Two individual mitochondria can undergo fusion, which consists in the merging of membranes and intramitochondrial contents, or fission, a process in which each mitochondrion divides itself into two smaller mitochondria. The overall balance between these opposing phenomena dictates mitochondrial number, length, degree of interconnection and even

functional properties such as respiratory capacity (Detmer and Chan, 2007). For instance, in respiratory active cells the mixing of mitochondrial gene products, enzymes and metabolites is beneficial, so mitochondria tend to present as an interconnected network (Malina, Larsson and Nielsen, 2018).

Mitochondria's localization within the cell varies according to cell type. In cells where ATP is highly consumed, mitochondria tend to localize near structures where this energy is needed, such as actin-myosin bundles involved in muscle contraction in muscle cells (Hermann and Shaw, 1998).

1.1. Structure and Function

Mitochondria are better known for their role in ATP production and their structure has clearly evolved towards maximizing the efficiency of this process. These organelles are bounded by highly specialized double membranes, the outer mitochondrial membrane (OMM) and the inner mitochondrial membrane (IMM), which create two distinct compartments with very different functions and constitutions, the intermembrane space and the mitochondrial matrix (Figure 1) (Karp, Iwasa and Marshall, 2015).

Acting as an external barrier, the OMM encloses the organelle from the cytosol. The presence of numerous molecules of porin, an integral transport protein, forms aqueous channels responsible for the permeability of this lipidic bilayer to large molecules up to 5000 Daltons (Da) (Alberts *et al.,* 2013). Due to these channels, the chemical composition of the intermembrane space regarding small molecules and inorganic ions is essentially equivalent to the cytosol. In contrast, the IMM is only permeable to molecules with a dedicated integral transport protein which means the contents of the mitochondrial matrix are highly specialized since molecules are selectively transported. This membrane can be subdivided in two domains with distinct functions and composed of different proteins. The first domain, called the inner membrane boundary, is in close proximity to the OMM and most likely participates in protein import (Detmer and Chan, 2007; Karp, Iwasa and Marshall, 2015). The second domain is located on the interior of the mitochondrion and forms a series of highly convoluted invaginations covering large surfaces, known as cristae, that contain the machinery required for aerobic respiration (Karp, Iwasa and Marshall, 2015; Rampelt *et al.*,

2017). These two domains are bounded to each other by narrow tubular connections, called cristae junctions (Karp, Iwasa and Marshall, 2015).

Both membranes have different properties associated with their functions (Figure 1). For instance, the OMM is involved in various biological processes such as oxidation of epinephrine and elongation of fatty acids, and therefore contains the enzymes needed for these processes. The IMM has a curious composition, being practically devoid of cholesterol and rich in an unusual phospholipid, cardiolipin, which is predominant in bacterial plasma membranes. This phospholipid facilitates the activity of several protein complexes involved in electron transport and ATP synthesis which are embedded in this membrane (Karp, Iwasa and Marshall, 2015).

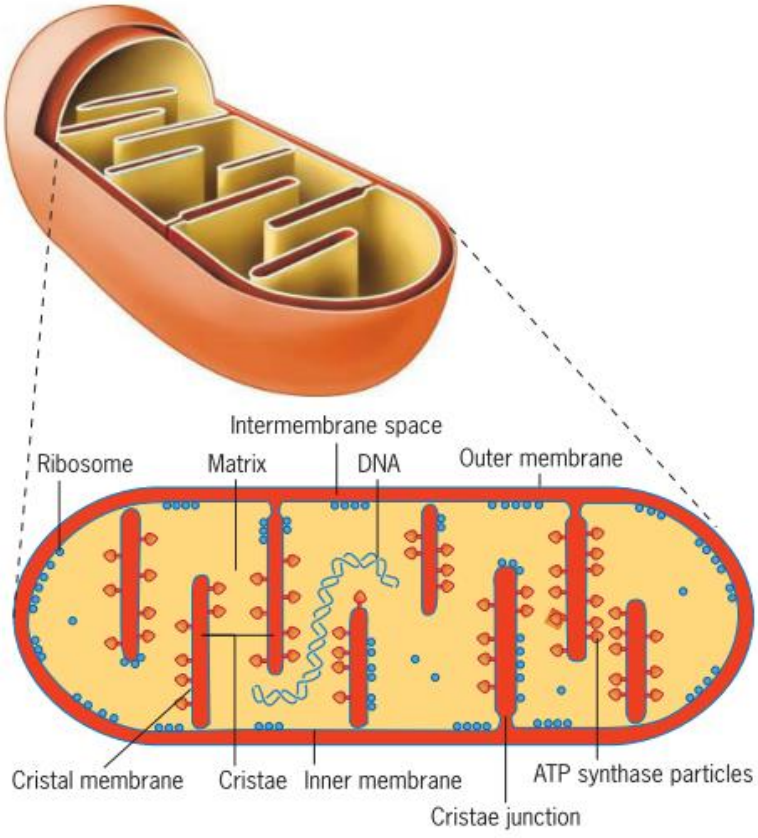

Figure 1 – Schematic representation of the three-dimensional internal structure of the mitochondria, shown from two different perspectives. Adapted from Karp, Iwasa and Marshall, 2015.

The mitochondrial matrix, presenting a gel-like consistency due to the high concentration of water-soluble proteins, also contains ribosomes and molecules of

mitochondrial DNA (mtDNA) (Karp, Iwasa and Marshall, 2015). This small circular genome is believed to be reminiscent of the ancient prokaryote that originated these organelles and is arranged into compact particles known as nucleoids (Detmer and Chan, 2007; Malina, Larsson and Nielsen, 2018). Currently, human mtDNA contains 37 genes, encoding 22 transfer RNAs, 2 ribosomal RNAs and 13 mitochondrial proteins involved in OXPHOS. Mitochondria use this machinery to translate 13 essential subunits of the enzyme complexes of the respiratory chain. The remaining subunits of these complexes are encoded by nuclear DNA (nDNA) (Larsson and Clayton, 1995; Wallace, Brown and Lott, 1999; Detmer and Chan, 2007; Malina, Larsson and Nielsen, 2018).

Although mitochondria are mostly studied because of their role in energy metabolism, these organelles are also involved in countless other cellular processes such as synthesis of amino acids, heme groups and fatty acids, ion homeostasis, regulation of calcium levels in the cytosol, production of oxygen reactive species, aging and apoptosis, just to name a few (Hermann and Shaw, 1998; Koopmman, Willems and Smeitink, 2012; Karp, Iwasa and Marshall, 2015).

1.1.1. Mitochondrial Disorders

The mitochondrion is a highly complex organelle involved in numerous essential processes within the cell. Therefore, mitochondrial dysfunction has implications in multiple cellular functions and results in a wide spectrum of human disorders (Lasserre *et al.*, 2015; Malina, Larsson and Nielsen, 2018). Mitochondrial diseases have been studied for at least 50 years, giving rise to the specialized field of mitochondrial medicine. To date, more than 150 genetic mitochondrial dysfunction syndromes have been described, and the majority is linked to defects in the mitochondrial energetic machinery, including in the respiratory chain (Lasserre *et al.*, 2015; Dautant *et al.*, 2018).

Mutations in mtDNA are frequent and result in mitochondrial dysfunction, causing a large array of clinically heterogeneous mitochondrial disorders associated with common pathologies such as cancer, diabetes mellitus, and cardiac disease, as well as neurodegenerative disorders such as Parkinson’s and Alzheimer’s disease (A. Johnson and Ogbi, 2011; Koopmman, Willems and Smeitink, 2012).

1.2. Oxidative Phosphorylation and the Respiratory Chain

The vast majority of cellular ATP in high eukaryotes, more than 90%, is produced in the mitochondria during oxidative phosphorylation (Højlund *et al.*, 2009; Biner *et al.*, 2018). OXPHOS is a highly conserved process in which nutrients, usually derived from fats and carbohydrates in the diet, are oxidized by enzymes to release their chemical energy, which is then used for ATP synthesis (Wallace, Brown and Lott, 1999; Dautant *et al.*, 2018). First, energy-rich nutrients are metabolized to acetyl-coenzyme A, which then delivers its acetyl group to the citric acid cycle to be oxidized into carbon dioxide, with the formation of NADH and $FADH_2$, which are cellular reduction equivalents (Biner *et al.*, 2018). These reduction equivalents are then oxidized to NAD^+ and FAD, and their electrons are transferred to the electron transport chain (Koopmman, Willems and Smeitink, 2012), also known as the respiratory chain , where they quickly pass along the chain and reduce molecular oxygen to water (Figure 2). The movement of electrons along the chain releases energy that is stored in the form of an electrochemical proton gradient, that is used to pump protons across the inner membrane, during ATP synthesis, in which the energy is converted into the phosphoanhydride bond of the ATP molecule (Alberts *et al.*, 2013; Biner *et al.*, 2018).

The redox reactions catalyzed in the respiratory chain are coupled to proton transfer from the matrix to the intermembrane space, generating a proton motive force composed of a pH and electrical differential across the membrane (Ackerman and Tzagoloff, 2005). This electrochemical gradient is used for ATP synthesis and other cellular processes such as import of proteins across the IMM. Loss of membrane potential can lead to arrested mitochondrial biogenesis and cell death (Ackerman and Tzagoloff, 2005).

The respiratory chain, present in countless copies, is embedded in the IMM and is composed of approximately 90 subunits divided into five enzymatic complexes (Larsson and Clayton, 1995; Biner *et al.*, 2018). The last complex of the respiratory chain, complex V, is also known as ATP synthase, an enzyme with a rotational mechanism that synthesizes cellular ATP using the electrochemical proton gradient. Mitochondrial DNA encodes only 13 subunits of the respiratory chain, including two subunits of complex V, ATP synthase, – ATP8 and ATP6 (Larsson and Clayton, 1995; Dautant *et al.*, 2018).

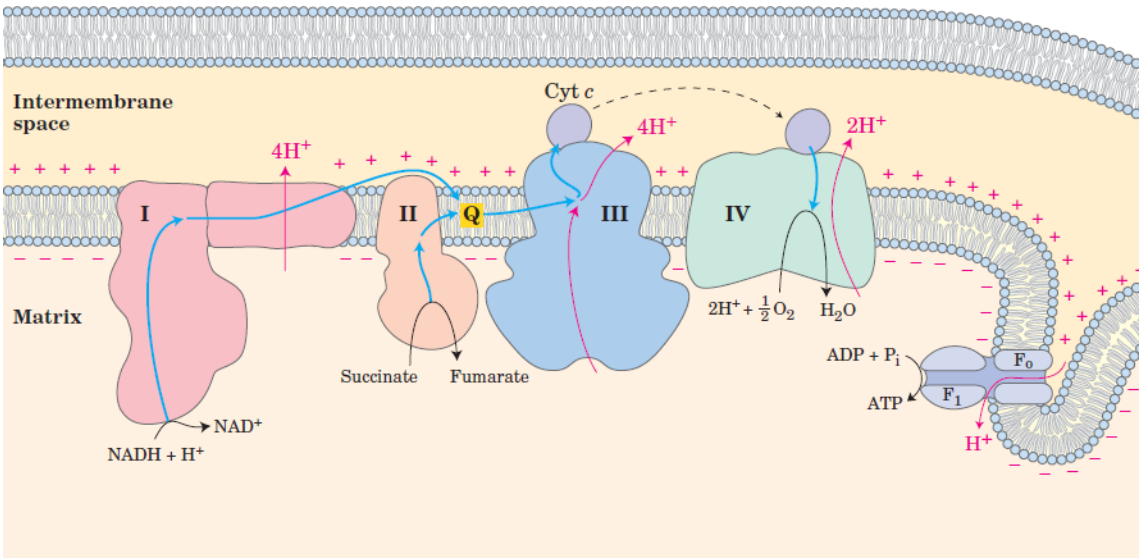

Figure 2 – Oxidative phosphorylation in mammals. Representation of mitochondrial OXPHOS, in which ATP synthesis is coupled to proton movement across the inner membrane. Electrons are transferred along the complexes of the respiratory chain, I through IV, reducing molecular oxygen to water, while protons are translocated against the gradient in the intermembrane space, by complexes I, III and IV. The proton motive force created leads to ATP synthesis, catalyzed by complex V, ATP synthase. (A). Scheme of the structure of mammalian ATP synthase, where both Fo and F1 domains are highlighted. Note: subunits A6L, e, f and g are omitted in this representation. Adapted from Nelson, Lehninger and Cox, 2008.

2. ATP Synthase – Overview

The electrochemical proton gradient is the driving force behind ATP synthesis, catalyzed by ATP synthase. This energy-generating enzyme has an ancient origin and is present in the plasma membrane of bacteria, in the chloroplasts of plants and algae as well as mitochondria of animal cells (Alberts *et al.*, 2013). Mitochondrial ATP synthase is encoded in both nuclear and mitochondrial genomes, but most subunits are encoded by nDNA, dispersed in separate chromosomes (Ackerman and Tzagoloff, 2005).

2.1. ATP Synthase – Structure

Mitochondrial ATP synthase, the primary site of ATP synthesis, is a large rotary protein complex, comprised of 13 different core subunits divided into two domains: a hydrophobic domain embedded in the membrane, Fo, and a soluble hydrophilic domain, F1, with a total approximate molar mass of 600 kDa (Kane and Van Eyk, 2009; Davies *et al.*, 2012; Karp, Iwasa and Marshall, 2015).

F1 domain, projected into the mitochondrial matrix, is composed of five different subunits with the stoichiometry α3β3γδε, all of them highly conserved and encoded by nDNA (Højlund *et al.*, 2009; Karp, Iwasa and Marshall, 2015). The γ, δ and ε subunits form a central stalk that connects the α3β3 hexamer to the membrane domain, Fo, and these are also connected via a peripheral stalk (Stock *et al.*, 2000). Fo domain contains the spanning subunits a and c, involved in proton translocation, in addition to subunits belonging to the peripheral stalk of the enzyme, involved in regulation of function and structure (Kane and Van Eyk, 2009). Fo also contains a channel through which protons are pumped (Karp, Iwasa and Marshall, 2015). In F1 domain, which is mainly involved in catalysis and regulation, α and β subunits are arranged alternately and the catalytic sites that bind adenosine diphosphate (ADP) and inorganic phosphate (Pi) are situated in each of the β subunits (Stock *et al.*, 2000; Højlund *et al.*, 2009; Kane and Van Eyk, 2009).

Cryo-EM structures of yeast and mammals show a similar subunit composition and structure as the human enzyme. The main differences being subunit c stoichiometry (8 in mammals, 10 in yeasts) and non-essential and yeast specific subunits, i and k (Dautant *et al.*, 2018).

2.2. ATP Synthase – Functions

ATP synthase is mainly known for its role in energy production but participates in several other cellular processes, including maintenance of the mitochondrial membrane potential – vital for the import of proteins into the mitochondria – and cristae structure, as well as participation in formation of the permeability transition pore and regulation of

cytochrome c mobilization during apoptosis (Scorrano *et al.*, 2002; Faccenda and Campanella, 2012; Long, Yang and Yang, 2015).

ATP synthesis occurs when protons are pumped, through the channel in Fo domain, from the intermembrane space into the mitochondrial matrix, which leads ATP synthase to rotate, using the driving force of the electrochemical proton gradient, and joining a molecule of Pi to a molecule of ADP, producing ATP (Alberts *et al.*, 2013; Long, Yang and Yang, 2015). However, ATP synthase is a reversible rotary complex and therefore, it can also hydrolyze ATP, if the protons are pumped in the opposite direction, for instance to maintain membrane potential (Long, Yang and Yang, 2015). So, ATP synthase catalyzes both synthesis and hydrolysis of ATP. F1 domain possesses three catalytic sites that, during ATP hydrolysis, transit through three different states with specific binding affinity for substrate and product. So, the binding of ATP to one site, promotes release of ADP + Pi from another. The same principle is true during ATP synthesis but, since the binding energy of ADP and Pi is too low to promote ATP release, energy from proton translocation through Fo is necessary (Ackerman and Tzagoloff, 2005).

Mitochondrial ATP synthase is usually present as a dimer, in the inner membrane cristae (Davies *et al.*, 2012). 3-D studies, namely electron microscopy tomography, revealed that mitochondrial cristae are tubular and pleomorphic (Frey and Mannella, 2000). These structures assure many functions including storage of cytochrome c reserves (Scorrano *et al.*, 2002) and optimization of mitochondrial respiration and ATP production (Rampelt *et al.*, 2017). Most of the OXPHOS machinery is embedded in the cristae membranes, which cover large surfaces, increasing respiratory efficiency. Abnormal cristae structure is associated with neurodegenerative disorders, highlighting the importance of cristae structure and dynamics for normal mitochondrial and cellular physiology (Rampelt *et al.*, 2017). As mentioned before, cristae connect to the inner membrane through tubular structures named cristae junctions, and the formation of both tubular cristae and cristae junctions is a dynamic process that has been associated with the dimerization of ATP synthase (Ackerman and Tzagoloff, 2005). ATP synthase dimers are arranged in rows alongside highly curved cristae ridges, which seem to play important roles in membrane morphology. Subunits e and g of ATP synthase were described as essential for the formation of yeast ATP synthase dimers (Paumard *et al.*, 2002; Davies *et al.*, 2012). In the absence of these subunits, mitochondria of yeast are devoid of cristae, showing digitations and onion-like structures instead (Paumard

et al., 2002; Ackerman and Tzagoloff, 2005). Additionally, rows of dimers constitute a pre-requisite for the formation of the typical highly convoluted lamellar cristae (Davies *et al.*, 2012). Mutations in subunits a and 8, of the peripheral stalk, are often correlated with pathological forms of mitochondrial cristae, which affect both ATP synthase function and the assembly process, as seen in the Leigh syndrome (Dautant *et al.*, 2018). Imaging of macromolecular complexes in their natural environment is essential to understand the role of ATP synthase in the dynamic morphologic changes of the IMM.

The inner mitochondrial membrane is highly selective and therefore mostly impermeable. However, under pathological conditions, the permeability of the mitochondrial membranes increases due to a phenomenon called mitochondrial permeability transition (MPT), characterized by the opening of a mitochondrial permeability transition pore (mPTP), which ultimately results in the swelling and death of the cell (Long, Yang and Yang, 2015). Opening of the mPTP also leads to release of cytochrome c from the IMM cristae into the cytosol and initiation of the intrinsic apoptotic cell death pathway (Detmer and Chan, 2007; Dave *et al.*, 2011). Recently, ATP synthase has been implicated in MPT-driven mitochondrial fragmentation, as well as cell death caused by accumulation of Ca^{2+} and oxidative stress, since its subunit c is a critical component of the mPTP (Long, Yang and Yang, 2015). Additionally, cyclosporine A has been found to bind OSCP and β subunits, indirectly inhibiting the c subunit mPTP pore due to a conformational change in ATP synthase, which causes F1 to be placed over said pore (Long, Yang and Yang, 2015). Other authors suggest dimers of ATP synthase may constitute the mPTP, in both mammals and yeast (Giorgio *et al.*, 2013; Carraro *et al.*, 2014). Although some evidence points towards ATP synthase being a key component of mPTP, many molecular and structural details remain unclear, so further studies are required.

2.3. ATP Synthase – Regulation

ATP synthase has been implicated in several human disorders such as cardiac conditions like heart failure, cardiomyopathy and preconditioning (Kane and Van Eyk, 2009; Long, Yang and Yang, 2015) as well as diabetes mellitus (Højlund *et al.*, 2009). So, understanding how regulation of ATP synthase affects energy metabolism is essential to

comprehend the mechanisms underlying these diseases, which could allow the identification of novel targets for treatment of these pathologies.

A nuclear-encoded inhibitor protein, the ATPase Inhibitory Factor 1 (IF1) regulates ATP synthase molecularly, inhibiting its hydrolytic activity that may occur upon loss of the electrochemical proton gradient across the inner mitochondrial membrane. IF1 localizes mainly in the mitochondrial matrix and interacts with the catalytic subunit of ATP synthase, β subunit, preventing hydrolysis of ATP and protecting cells from damage caused by ATP depletion (Faccenda and Campanella, 2012; Long, Yang and Yang, 2015). IF1 is the only ATPase inhibitor protein in bovine mitochondria, but yeast mitochondria have two inhibitory peptides, Inh1p and Stf1p. These peptides display different binding affinities despite being homologous in yeast (Ackerman and Tzagoloff, 2005). Bovine IF1 is also involved in dimerization of ATP synthase, since IF1 dimerizes in conditions of maximal binding to ATP synthase, placing F1-interaction domains at opposing ends of the molecule (Ackerman and Tzagoloff, 2005; Faccenda and Campanella, 2012). Consistent with this hypothesis, F1:IF1 complexes were shown to be dimeric (Cabezón *et al.*, 2000), so IF1 has also been implicated in remodeling of cristae structure and consequent regulation of morphology and mito-ultrastructure (Faccenda and Campanella, 2012). Overexpression of IF1 is associated with human carcinomas and differences in ratio of expression between ATP synthase and IF1 alter the cellular response to ischemia/reperfusion injury (Willers and Cuezva, 2011; Faccenda and Campanella, 2012).

Controlling translation of RNA by regulatory RNA binding proteins is another way in which ATP synthase is regulated. Studies show that, in yeast, the mRNA encoding β subunit of ATP synthase is usually sorted by the 3′-Untranslated Region (3'UTR) to the vicinity of the mitochondria. Deletion of 3'UTR from the ATP2 gene has several biological implications including deficient protein import, mtDNA depletion, diminished ATP synthesis and respiratory dysfunction (Willers and Cuezva, 2011). Human β-mRNA has been shown to associate with Ras-GAP SH3 binding protein 1 (G3BP1), namely via its 3'UTR, which leads to a repression in mRNA translation by preventing the recruitment of mRNA into active polysomes. It is suggested that binding of G3BP1 to the 3'UTR region may obstruct the intrinsic translational activity of the 3'UTR, hindering either mRNA circularization or 43S recruitment to the mRNA. G3BP1 overexpression in human cells

results in inhibition of synthesis of β-F1- ATPase with no alteration in the levels of β-mRNA, and G3BP1 overexpression is frequent in cancer cell lines (Willers and Cuezva, 2011).

Since the cellular energy requirements fluctuate rapidly, ATP synthase activity must be regulated by several dynamic regulatory elements at the enzyme level (Long, Yang and Yang, 2015). Mitochondrial Ca^{2+} has been implicated in the regulation of ATP synthase activity, but the mechanisms involved are still unclear. Early studies suggest involvement of a protein named calcium-binding ATPase inhibitor (CaBI) which depends on Ca^{2+} to interact with ATP synthase, simultaneously promoting the synthesis and preventing the hydrolysis of ATP (Long, Yang and Yang, 2015).

2.3.1. Phosphoregulation of Mitochondrial Proteins

Biological processes are also regulated via post-translational modifications (PTM). PTMs have been studied for decades and there are numerous different types such as acetylation, phosphorylation, nitration, hydroxylation, among many others (Agnetti *et al.*, 2007). However, phosphorylation is by far the most common post-translation way to regulate protein function (Ohlmeier, Hiltunen and Bergmann, 2010).

The development of methods specific for detection of PTMs, such as selective dyes, antibodies and mass spectrometry (MS)-based approaches, have resulted in the detection of numerous PTMs in all subunits of ATP synthase. These include not only phosphorylation and acetylation, which are rather common, but also trimethylation, nitration, s-nitrosylation and tryptophan oxidation, which occur sporadically (Kane *et al.*, 2010; Long, Yang and Yang, 2015). Nonetheless, the biological significance for most of these PTMs is still unknown. Since phosphorylation is a rapid and reversible way to regulate protein stability, conformation, interaction and enzymatic activity, it is often studied in mammalian systems (Kane and Van Eyk, 2009; Huttlin *et al.*, 2010; Ohlmeier, Hiltunen and Bergmann, 2010).

Phosphorylation is a reversible modification in which a phosphoryl group is attached to a protein substrate. Protein phosphorylation occurs when a phosphoryl group is covalently attached by a protein kinase to a protein substrate, which results in changes of the structural conformation of the protein. The reverse process is known as dephosphorylation and is carried out by a protein phosphatase (Cheng *et al.*, 2011).

Until recently the mitochondrial proteome was believed to be un-phosphorylated because of the mitochondria's double membrane system. However, studies confirm that the mitochondrial proteome is, indeed, much more phosphorylated than anticipated, reporting approximately 9400 phosphorylation sites in 972 proteins in yeast mitochondria (Frankovsky *et al.*, 2021). Hopper *et al.* characterized the phosphoproteome of mitochondria in pig heart, using two-dimension gel electrophoresis (2DE) and radioactive phosphorus-32 (^{32}P) labeling analysis, identifying 45 proteins involved in different metabolic pathways, such as reactive oxygen species metabolism or oxidative phosphorylation, including the β subunit of ATP synthase (Hopper *et al.*, 2006).

In *Saccharomyces cerevisiae*, nDNA encodes at least 130 kinases and 40 phosphatases. Numerous protein kinases and phosphatases have been observed in proteomics analysis of isolated mitochondria as well as in ^{32}P studies, supporting the idea that mitochondrial processes are indeed regulated by reversible phosphorylation (Reinders *et al.*, 2007). So far, hundreds of phosphosites in mitochondrial proteins have been described (Covian and Balaban, 2012; Frankovsky *et al.*, 2021) but the majority of regulatory kinases and phosphatases involved remains to be identified (Nowak and Bakajsova, 2015).

2.3.2. Phosphorylation of ATP Synthase

The mitochondrial respiratory chain is composed of five distinct complexes and studies show that subunits in all of them are phosphorylated thus potentially regulated by kinases and phosphatases localized to the mitochondria (Højlund *et al.*, 2009). ATP synthase is extremely important in the energy-producing pathway, but the regulation of its activity is not yet fully understood.

The advances and optimization of PTM-specific MS-based methods, in addition to selective antibodies and novel reagents like Pro-Q Diamond gel stain, allowed the detection of numerous PTMs in subunits of ATP synthase (Kane and Van Eyk, 2009). In mammalian systems, several phosphorylation sites have already been identified in this protein complex and most of them are located in the catalytic domain, F1 (Figure 3) (Covian and Balaban, 2012). However, the biological function of most of these PTMs remains to be uncovered, as

well as the functional impact in pathological conditions (Kane and Van Eyk, 2009; Covian and Balaban, 2012).

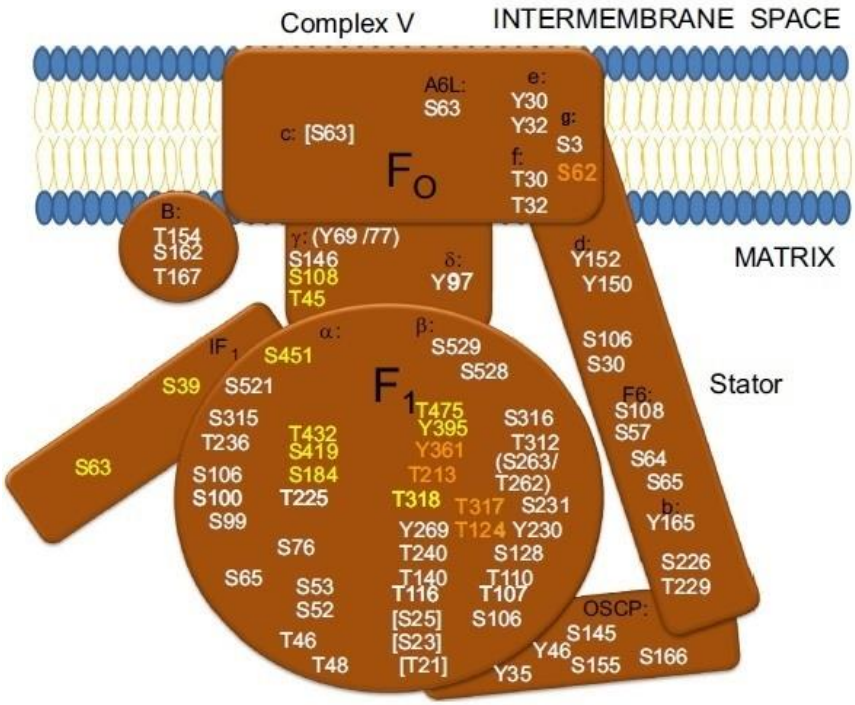

Figure 3 – Reported phosphorylated residues of ATP synthase. In this image, residues in the designated region and subunit are shown in different colors according to the functional effect that results of its phosphorylation. Sites are written in white if no functional effect has been described and their location within the structure does not suggest impact on activity. Residues colored in yellow could affect activity based on their location in the structure, but do not have described functions. Lastly, the sites that, based on structure, could influence function, and have been described as having altered phosphorylation levels in different physiological states, are shown in orange. In brackets, are the sites located in the pre-sequence and absent in the fully assembled complex. Adapted from Covian *et al* 2012.

The phosphorylation of β subunit has been studied in different tissues and organisms, namely pig heart and liver, human skeletal muscle, rabbit ventricular myocytes, and yeast, among others (Covian and Balaban, 2012). Even though the phosphatase/kinase system involved is still unclear, several phosphorylation sites in the β subunit have been described (Figure 3), however, several are distant from the catalytic site and therefore seem to have no impact on the activity of the complex (Covian and Balaban, 2012).

Using an improved detection method combining optimized IMAC – immobilized metal affinity chromatography – for isolation of phosphopeptides and MS^3 (MS/MS/MS) for

phosphopeptides fragmentation, Lee *et al.* reported 84 phosphorylation sites from 62 proteins, in mitochondria from mouse liver, including a C-terminal serine, Ser529, of FoF1 ATP synthase β subunit (ATPsyn-β) (Lee *et al.*, 2007). Using intact mitochondria from human skeletal muscle, Zhao *et al.* showed that ATPsyn-β is phosphorylated at the residues Thr213, Ser529 and Ser415 (Zhao *et al.*, 2011).

Using a combination of MS and enrichment strategies to analyze isolated yeast mitochondria, Reinders *et al*. identified two phosphorylation sites in the g subunit of ATP synthase, Ser3 and Ser62, and demonstrated that phosphorylation of Ser62 is involved in the regulation of ATP synthase dimerization (Reinders *et al.*, 2007).

Højlund *et al.* studied the relation between phosphorylation in healthy and insulin-resistant skeletal muscle, in humans, with the goal of identifying phosphorylation sites of ATPsyn-β (Højlund *et al.*, 2009). Using a targeted MS/MS strategy, the authors reported five new phosphorylation sites in human ATPsyn-β, Thr475, Tyr230, Tyr269, Tyr361 and Tyr395. The authors also observed phosphorylation of Thr213 and Thr312, previously reported as phosphorylation sites. Interestingly, Thr213 is located in the nucleotide-binding region of ATPsyn-β (Højlund *et al.*, 2009). Basal phosphorylation increased approximately 30% in two residues, Thr213 and Tyr361, for obese non-diabetic participants and type 2 diabetics, compared with lean healthy individuals. There is a possibility, supported by this data, that the activity of ATP synthase may be regulated by reversible phosphorylation at specific serine/threonine/tyrosine residues, since phosphorylation of residues within its catalytic site interferes with the binding of Pi and ADP, affecting ATP synthesis. Immunoblotting revealed a tendency for the decrease of protein levels of ATPsyn-β from lean individuals to obese non-diabetic participants to type 2 diabetic individuals. This decreasing trend in protein levels was mirrored by other complexes of the respiratory chain such as complex I, II and III as well as ATP synthase α subunit, for obese and diabetic patients, compared to lean healthy participants (Højlund *et al.*, 2009). Overall, these results suggest that phosphorylation of human ATPsyn-β in skeletal muscle may play an important regulatory role in ATP synthesis and complications within this pathway, combined with reduced levels of OXPHOS proteins, may contribute to type 2 diabetes (Højlund *et al.*, 2009). Thus far, the kinases and phosphatases involved in the regulation of these phosphosites have not been identified.

Phosphorylation in the β subunit of ATP synthase was also found to occur in preconditioned myocardium of rabbit ventricular myocytes. Using a 2DE approach combined with MS/MS, five novel phosphorylation sites were identified, Ser106, Thr107, Thr262/Ser263, Thr312 and Thr368, and each of these sites is conserved across mammalian species (Arrell *et al.*, 2006). Interestingly, x-ray crystal 3D structure of the complex shows that two of these phosphorylated residues, Thr312 and Thr368, are inaccessible in the fully assembled complex, suggesting that phosphorylation of these residues occurs before assembly. The three remaining residues are accessible in the fully assembled complex, which makes them candidates for dynamic regulation. Studies using a rat heart model also showed a correlation between ATP synthase and cardiac preconditioning, since the protective effect of ischemia is associated with lower levels of ATP synthase activity (Arrell *et al.*, 2006). Follow-up studies were performed, using *S. cerevisiae* as a model, to evaluate the functional consequences of Atp2 phosphorylation (Kane *et al.*, 2010). Only four out of five residues have homologs in yeast: Ser106 (Thr58), Thr262/Ser263 (Ser213), Thr312 (Thr262) and Thr368 (Thr318) and each residue was mutated into alanine (phosphoresistant) or aspartic and glutamic acid (phosphomimetics). Results show that mimicking phosphorylation of Thr262 hinders ATPase function of the complex and simulating phosphorylation of Thr58 affects mainly dimer formation, suggesting an additional role for Atp2 phosphorylation in the regulation or maintenance of dimerization (Kane *et al.*, 2010). This study confirms that the phosphorylation of these conserved residues, previously identified in rabbit heart, impacts both structure and function of the ATP synthase complex. Additional studies have described complex V-associated effects on cardiac preconditioning, but the common denominator seems to be attenuation of ATPase activity of the complex, which could decrease FoF1 ATPase-mediated ATP hydrolysis during prolonged ischemia (A. Johnson and Ogbi, 2011).

Studying the phosphoproteome of Arabidopsis, Reiland *et al.* reported phosphorylation of the β subunit of the ATP synthase of chloroplast, which is identical to the mitochondrial ATP synthase (Reiland *et al.*, 2009). These authors evaluated dynamics of phosphorylation during the circadian cycle, by analyzing samples collected at the end of day and at the end of night. Results of this study confirm that ATP synthase activity is regulated via phosphorylation since phosphorylation of β subunit of the ATP synthase was the only phosphorylation event reproducibly observed (Reiland *et al.*, 2009). A casein kinase

II-like enzyme has been suggested to phosphorylate the β subunit of ATP synthase of chloroplast, in spinach tissue but the phosphorylation sites have not been identified (Kanekatsu *et al.*, 1998; Reiland *et al.*, 2009).

Protein kinase C isozymes are involved in mechanisms of cardiac preconditioning and some studies suggest that PKC isozymes may modulate FoF1 ATP synthase functions (Agnetti *et al.*, 2007; A. Johnson and Ogbi, 2011). A phosphoproteomics study reported that activation of protein kinase C δ (PKCδ) results in the phosphorylation of subunits α and β of the ATP synthase in rat tissue (Dave *et al.*, 2011). In this study, which aimed to identify mitochondrial targets of translocated PKCδ, isolated mitochondria were evaluated after treatment with PKCδ activator peptide (ΨRACK) or tat carrier peptide (control), resulting in the identification of 18 proteins (Dave *et al.*, 2011). In addition, cardiac myocytes were protected from injury in the presence of a PKCδ translocation inhibitor. This inhibitor also improved recovery of ATP levels, when administered immediately after prolonged ischemia in mouse hearts, during oxygenated reperfusion (A. Johnson and Ogbi, 2011). Studies attributed this protection to a relief mediated by a PKCδ inhibitory effect on the FoF1 ATP synthase complex, which involves a direct binding interaction between PKCδ and subunit d of the ATP synthase complex (Nguyen, Ogbi and Johnson, 2008). Another isoform, protein kinase C α (PKCα), is involved in phosphorylation of the c subunit of ATP synthase after treatment with a kidney-damaging environmental toxin. *In vitro,* PKCα directly phosphorylates subunit c, decreasing ATP synthase activity (Nowak and Bakajsova, 2015). PKCα dependent phosphorylation of ATP synthase has been associated with improved mitochondrial respiration following cellular injury caused by hypoxia and reperfusion or exposure to toxins (Castellanos and Lanning, 2019). Further studies are required to evaluate the functional significance of the phosphorylation in all complexes of the respiratory chain, especially ATP synthase, the main producer of cellular ATP. These studies should include the contributions of kinases and phosphatases involved in the phosphorylation of OXPHOS machinery (Castellanos and Lanning, 2019).

Pereira *et al.* investigated the regulation of mitochondrial proteins by Sit4p, a type 2A-related phosphatase. Sit4p participates in a large array of cellular functions including nutrient signaling, glucose and lipid metabolism and control of G1 cyclin genes, among others (Pereira *et al.*, 2018). It was found that deletion of *SIT4* caused increase in the phosphorylation status of 9 mitochondrial proteins, including subunits α and β of the ATP

synthase complex, which is well-conserved (Pereira *et al.*, 2018). Atp2p, which showed the biggest extent in phosphorylation, was further characterized and two phosphorylation sites were identified, Thr124 and Thr317. Both residues are highly conserved across species. These studies indicated Sit4 may directly dephosphorylate Atp2, thus being the first phosphatase described to regulate ATP synthase phosphorylation. Thr124 is situated close to the matrix-facing portion while Thr317 is located close to the center of the complex, suggesting that phosphorylation occurs before complex assembly (Figure 4). Phosphorylation of these residues was shown to increase Atp2p stability leading to an increase in protein levels not only of Atp2, but the whole ATP synthase complex (Pereira *et al.*, 2018). Furthermore, mimicking phosphorylation at these sites, resulted in increased ATP synthase activity, mitochondrial respiration and cellular ATP content. Curiously, human Atp2p homologue, ATPsyn-β, has been shown to be phosphorylated at the correspondent threonine residues (hThr140 and hThr334, respectively), implying conservation of this post-translation regulation.

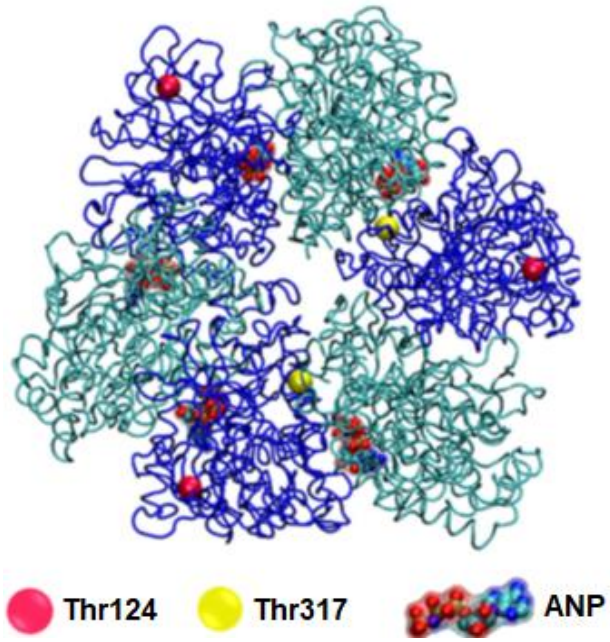

Figure 4 – Phosphorylated residues, Thr124 and Thr317, plotted in the 3D structure of the ATP synthase α/β hexamer. Light blue ribbons represent α subunit, dark blue ribbons represent β subunit and ATP binding pocket is represented by the phosphoaminophosphonic acid-adenylate ester ATP-analog (ANP). Adapted from Pereira *et al.*, 2018.

2.3.2.1. Methods for the Detection of Phosphorylation

Numerous techniques have been employed in the detection of protein phosphorylation and these methods are constantly improving. The most common approaches include 2DE followed by different staining techniques (Coomassie, silver staining, SYPRO Ruby, etc), ^{32}P labeling and proteomic analysis, namely MS analysis. Other methods involve phosphoprotein stains like Pro-Q Diamond, that binds to proteins containing phosphate, or antibodies that recognize phosphoproteins, that is, antibodies specific for phospho-serine, phospho-threonine or phospho-tyrosine. Enzymatic dephosphorylation, by usage of phosphatase assays can also be used to identify phosphorylation, since removing phosphate groups causes alterations in the protein charge after treatment (Agnetti *et al.*, 2007).

The use of phospho-specific antibodies is still somewhat risky since the successful detection is largely dependent on the sensitivity and affinity of the antibody employed to the phosphoprotein of interest. In addition, specific antibodies for novel phosphorylated residues are not commercially available.

Another common approach, as mentioned before, is the separation of proteins and its modified forms by 2DEs, in which proteins are separated first according to their isoelectric points (IP), and second according to their molecular weight. Phosphorylation should lead to an alteration in the protein IP. Yet, since other modifications, like acetylation, also cause IP shifts, 2DE separation must be followed by immunoblotting with anti-phospho antibodies to identify the phosphorylated forms as in Pereira *et al.*, 2018 for Atp2.

A novel method for detection of phosphorylation is Phos-Tag™ SDS-PAGE (Wako, 2016). A functional molecule binds phosphorylated residues, causing them to migrate slower, and separating proteins accordingly to their phosphorylation status. Since it is quick and easy to perform, allows simultaneous analysis of several samples and requires very common laboratory equipment, this method has several advantages over its competitors.

3. *Saccharomyces cerevisiae* as a Model Organism

A lot of what we know about mitochondrial function, including regulation, key processes, components and interplay with cellular functions, derives from studies using *S. cerevisiae* (Lasserre *et al.*, 2015). Thus, budding yeast has become the preferred model organism to study mitochondrial dynamics since this process has many similar aspects to other cell types (Hermann and Shaw, 1998; Sierra *et al.*, 2015). Yeast cells, unlike cells of other organisms, are viable with impaired or even disrupted oxidative phosphorylation and without functional mtDNA, provided they have a fermentable carbon source. This allows the study of mitochondrial dysfunction, analysis of several mutations and characterization of the corresponding genes (Lasserre *et al.*, 2015; Sierra *et al.*, 2015; Malina, Larsson and Nielsen, 2018) . Since the majority of mitochondrial functions is maintained across eukarya, using budding yeast as a model system may provide new perspectives on several human diseases (Malina, Larsson and Nielsen, 2018). There are evidences supporting that approximately 30% of genes implicated in human disease have orthologs in baker's yeast and about 70% of nuclear genes implicated in mitochondrial disorders are conserved amongst yeast and humans (Karathia *et al.*, 2011; Lasserre *et al.*, 2015; Malina, Larsson and Nielsen, 2018).

Yeast models present advantages in the study of mitochondrial function. The yeast genome has been fully sequenced and its annotation is incredibly thorough (Lasserre *et al.*, 2015). *S. cerevisiae* as a unicellular organism is amenable to genetic and chemical screening (Lasserre *et al.*, 2015). In addition, yeast populations share copies of mtDNA with the same sequence after a few generations, becoming homoplasmics and allowing the assessment of point mutations that are usually heteroplasmics in human mitochondria, elucidating the molecular basis of these diseases' pathogenicity (Dautant *et al.*, 2018; Malina, Larsson and Nielsen, 2018).

S. cerevisiae was used in several studies of ATP synthase since this protein is conserved. For instance, human and yeast ATP synthase share an almost identical composition of its subunits, accentuating the value of using yeast as a model to uncover useful information relevant in higher eukaryotes (Ackerman and Tzagoloff, 2005). The study of diseases associated with ATP synthase, such as those caused by mutations in mitochondrial MT-ATP6 and MT-ATP8 genes, is challenging due to factors such as variable

penetrance and complex inheritance. In this context, the use of yeast provides a new level of understanding of how these mutations affect ATP structure, assembly and mechanism (Dautant *et al.*, 2018).

Finally, yeast genes, both nuclear and mitochondrial, can easily be mutated, deleted, and reintroduced into yeast cells, as well as overexpressed and tagged, which allows researchers to gather vital information to uncover the molecular basis of diseases (Foury, 1997).

4. Objectives

In recent years, it has been shown that ATP synthase is subject to regulation via post-translation modifications, namely phosphorylation. Pereira *et* al. uncovered a physical and genetic relation between the Sit4 phosphatase and the β subunit of ATP synthase, which ultimately led to the identification of two phosphorylated peptides: Thr124 and Thr317 (Pereira *et al.*, 2018). Interestingly, phosphorylation of the human homologues Thr140 and Thr334, respectively, has also been reported. In *S. cerevisiae*, phosphorylation of these residues leads to increased Atp2p phosphorylation and overall increased ATP synthase activity. However, the kinases involved in the regulation of these residues, either in yeast or in mammals, are unknown.

Using *S. cerevisiae* as a model, the goal of this project was to identify kinase(s) involved in the phosphoregulation of the β subunit (Atp2p) of FoF1 ATP synthase, to improve our understanding of the regulation of this essential enzyme. To do so, bioinformatics tools were used to predict kinase regulators, by examining kinase consensus sites. Strains overexpressing hit kinases were constructed and their effect on Atp2p phosphorylation evaluated using Zn^{2+}Phos-Tag™ SDS-PAGE. Atp2p levels upon kinase overexpression were also evaluated, as Atp2p phosphorylation was associated with increased protein levels. Additionally, the effect of the most promising candidate on mitochondrial respiration and respiratory growth was analysed.

2. Materials and Methods

2.1. Plasmids and Yeast Strains

All *Saccharomyces cerevisiae* strains used in this study are in a BY4741 yeast strain background (S288c derived) and are listed in Table 1, along with the plasmids that were used.

Table 1 - Saccharomyces cerevisiae strains and plasmids used in this study.

Strain	Genotype	Source
	S. cerevisiae	
BY4741 (wild type)	MATa *his3Δ1 leu2Δ0 met15Δ0 ura3Δ0*	EUROSCARF
Cdc28^{td}	[BY4741] *cdc28-td::KanMx4* Orf YBR160W	EUROSCARF (Dohmen 1994)
p*MET25*-Pkc1	[BY4741] NatNT2-*MET25*-3HA-*PKC1*	This study
p*MET25*-Ipl1	[BY4741] NatNT2-*MET25*-3HA-*IPL1*	This study
p*MET25*-Cdc5	[BY4741] NatNT2-*MET25*-3HA-*CDC5*	This study
p*MET25*-Hrr25	[BY4741] NatNT2-*MET25*-3HA-*HRR25*	This study
p*GAL*-Hrr25-degron	[BY4741] pRS315-*PGAL*-3HA-*HRR25*-Degron	This study
pTs-842	[BY4741] *pTs-842*	This study
p*GAL1*-Cdc5	[BY4741] KanMx6-*pGAL1-3HA-CDC5*	This study
Atp2-wt	[BY4741] *atp2Δ::*kanMx4 + pRS316-*ATP2*	Pereira *et al*., 2018
Atp2-Thr124A	[BY4741] *atp2Δ::*kanMx4 + pRS316A-*ATP2*-Thr124A	Pereira *et al*., 2018
Atp2-Thr317A	[BY4741] *atp2Δ::*kanMx4 + pRS316A-*ATP2*-Thr317A	Pereira *et al*., 2018
Atp2-Thr124A/Thr317A	[BY4741] *atp2Δ::*kanMx4 + pRS316A-*ATP2*-Thr124A/Thr317A	Lab collection
Δ*atp2*	[BY4741] *atp2Δ::*MxHIS3	Lab collection
Δ*atp2* p*GAL1*-Cdc5	[BY4741] *atp2Δ::*MxHIS3 KanMx6-*pGAL1*-3HA-*CDC5*	This study
Δ*atp2* p*GAL1*-Cdc5 [pRS316- ATP2]	[BY4741 *atp2Δ::MxHIS3* KanMx6-*pGAL1*-3HA-*CDC5* + pRS316-*ATP2*	This study
Δ*atp2* p*GAL1*-Cdc5 [pRS316- ATP2-Thr124A/Thr317A]	[BY4741] *atp2Δ::MxHIS3* KanMx6-*pGAL1*-3HA-*CDC5* + pRS316A-*ATP2*-Thr124A/Thr317A	This study
	Plasmids	
MET25	MET25pr-3HA NAT-NT2	Lab collection
GAL1	pFA6a-kanMX6-PGAL1-3HA	Lab collection
HRR25-Degron	pKK204 (pGAL-3HA-Hrr25-degron)	Kafadar *et al*. 2003
pTs-842	pTS842 (degron vector)	Kafadar *et al.* 2003

2.2. Construction of Yeast Mutants

2.2.1. Polymerase Chain Reaction Conditions

DNA cassettes used to construct yeast mutants were amplified by polymerase chain reaction (PCR), performed in a T100™ Thermal Cycler (Bio-Rad) with a heated lid. The used procedures are described below, as well as the PCR programs and primers (Table 2).

PCRs for cassette amplification were routinely performed in 40µL reaction mixes containing 0.5µM sense primer, 0.5µM anti-sense primer, 20µL Supreme NZYTaq II 2x Green Master Mix (NZYtech genes & enzymes) and appropriate amount of plasmid and water for the desired final volume.

PCRs for strain construction confirmation were routinely performed in 20µL reaction mix containing 0.25µM sense primer, 0.25µM anti-sense primer, 10µL Supreme NZYTaq II 2x Green Master Mix (NZYtech genes & enzymes) and 8µL of cell suspension. Cell lysis was accomplished by heating the cell suspension in a microwave oven for approximately 30 seconds, before adding the reaction mix.

PCR products were examined by nucleic acid electrophoresis at 120V for 30 minutes, using 0.8-1% agarose gels containing GreenSafe Premium 0.04µL/mL (NZYtech genes & enzymes) and TAE buffer (40mM Tris, 20mM acetic acid, 1mM EDTA). DNA bands were detected upon UV fluorescence, and when necessary, excised from the gel and purified using NZYGelpure kit (NZYtech genes & enzymes). DNA was quantified using Nanodrop 1000 (ThermoFisher Scientific).

Table 2 - Primers and respective PCR programs used in this study.

Gene	Primer	Nucleotide sequence	PCR program		
			Annealing Temperature	Extension Time (s)	Number of Cycles
***MET25*-CDC5 amplification**	CDC5 S1MetF	AATCACAGCCGTGGAGAAGAAAGA ACAGAGTAAGATCAAGTCGAATAA AG*ATGCGTACGCTGCAGGTCGAC*	54 °C	90 (10 cycles) 90 + 20s per cycle (22 cycles)	32
	CDC5 S4MetR	CTTGGAACGGGTATTCAATTGCTTA TCATTGATAGCTTTAAGAGGACCC AACGA*CATCGATGAATTCTCTGTCG* TGATGATCATTATTCGGATCTAG			
***MET25*-CDC5 confirmation**	CDC5 Conf_F	GTGGAGAAGAAAGAACAGAG	47 °C	90 (10 cycles) 90 + 20s per cycle (22 cycles)	32
	CDC5 Conf_Rvs	TGATGATCATTATTCGGATCTAG			
***MET25*-HRR25 amplification**	HRR25 S1MetF	AAAAACCAAAAAGAAAAGATATAT TTATAGAAAGGATACATTAAAAAG AGATGCGTACGCTGCAGGTCGAC	54 °C	90 (10 cycles) 90 + 20s per cycle (22 cycles)	32
	HRR25 S4MetR	CCACTCCCAATCTTCCTGCCAATAC GAAATTTCCTTCCTACTCTTAAGTC CATCGATGAATTCTCTGTCG			
***MET25*-HRR25 confirmation**	HRR25 Conf_F	GCATCTTTAAACCTCTGTTGGGT	52 °C	90 (10 cycles) 90 + 20s per cycle (22 cycles)	32
	HRR25 Conf_Rvs	GTGCCGTGGTAAATGTCACC			
***MET25*-IPL1 amplification**	IPL1 S1MetF	AAAAAAAACTGGGATTTTGAAATA CAACAAAAGAAAGAAGTAAAAAG GGAATGGTACGCTGCAGGTCGAC	54 °C	90 (10 cycles) 90 + 20s per cycle (22 cycles)	32
	IPL1 S4MetR	TTCGATGGCGAATTAGCGTTTAGTT TGATATTTACTAAACTATTGCGTTG CATCGATGAATTCTCTGTCG			
***MET25*-IPL1 confirmation**	IPL1 Conf_F	AGCAAGATCATTCTTAGCGC	50 °C	90 (10 cycles) 90 + 20s per cycle (22 cycles)	32
	IPL1 Conf_Rvs	CTGCGGCGAATGGGATATTC			
***MET25*-PKC1 amplification**	PKC1 S1MetF	GCGAGGAAAAGTAAGTATAGTATC ACACATATAGGGAGCAGTTTACAG TCATGCGTACGCTGCAGGTCGAC	54 °C	90 (10 cycles) 90 + 20s per cycle (22 cycles)	32
	PKC1 S4MetR	TCTTCGACGGCTATCTTTTTTTTAA TGTTCTGCTCCAATTGTGAAAAACT CATCGATGAATTCTCTGTCG			
***MET25*-PKC1 confirmation**	PKC1 Conf_F	AACCTAGAACAGTAGCTG	46 °C	90 (10 cycles) 90 + 20s per cycle (22 cycles)	32
	PKC1 Conf_Rvs	GACCATAACATTGCTAGTC			
p*GAL1*-CDC5 amplification	CDC5_F4	CACAGCCGTGGAGAAGAAAGAAC AGAGTAAGATCAAGTCGAATAAAG *ATG*GAATTCGAGCTCGTTTAAAC	47 °C – 5 cycles 60 °C – 30 cycles	90	35
	CDC5_R3	CGGGTATTCAATTGCTTATCATTGA TAGCTTTAAGAGGACCCAACGAGC ACTGAGCAGCGTAATCTG			
p*GAL1*-HRR25 amplification	HRR25_F4	GGTGAAAACACATCTTAGTAGCAT CTTTAAACCTCTGTTGGGTACTTAG ATGGAATTCGAGCTCGTTTAAAC	65 °C – 5 cycles 60 °C – 30 cycles	90	35
	HRR25_R3	CCACTCCCAATCTTCCTGCCAATAC GAAATTTCCTTCCTACTCTTAAGTC GCACTGAGCAGCGTAATCTG			

2.2.2. Yeast Transformation

Yeast strains were transformed according to the standard lithium acetate/single-stranded carrier DNA/ polyethylene glycol method, described by Gietz (Gietz and Schiestl, 2007).

Briefly, cells were grown overnight in YPD until early logarithmic phase (OD_{600}=0.4). Then, 10mL of cells were pelleted, washed, resuspended in 1mL of sterile water and transferred to a microtube. Cells were then incubated with the transformation mix, composed of 240µL of 50% (w/v) polyethylene glycol 3350 freshly made, 36µL 1M lithium acetate, 25µL 5 mg/mL boiled single-stranded DNA, 1mg DNA cassette or 200ng plasmid DNA (pDNA) and sterile water to complete the final volume of 360µL, assuring thorough homogenization. An aliquot with water instead of DNA was used as a negative control for every transformation. Cells were incubated at 26 °C for 30 minutes followed by 30 minutes at 42 °C. After incubation, cells were gently transferred to selective media and allowed to recover at 26 °C for 4-5 hours on an orbital shaker. Finally, cells were pelleted, resuspended in 100µL of sterile water and plated in the appropriate selective media. For transformations using pDNA the incubation period of 30 minutes at 26 °C was omitted as well as the recovery period. Plates were incubated at 26 °C for 2-4 days to obtain transformants. Resistant colonies were re-streaked on selective media plates.

The correct insertion of the *MET25* and *GAL1* promoters was confirmed by PCR, using the primers and conditions listed in Table 2. Transformants were also confirmed by Western Blotting analysis by probing for HA.

2.3. Growth Conditions

Yeast strains were grown in aerobic conditions at 26 °C on an orbital shaker at 140 revolutions per minute (rpm) and the ratio between flask volume and growth medium was 5:1. Optical density was measured at 600nm (OD_{600}) using a Shimadzu UV-2401 PC spectrophotometer and cells were routinely grown to early exponential phase (OD_{600}=0.5).

Liquid growth media consisted of rich medium [YPD – Yeast Peptone Dextrose – 1% (w/v) yeast extract (Liofilchem), 2% (w/v) bactopeptone (Liofilchem) and 2% (w/v)

glucose (Liofilchem)); YPGal – Yeast Peptone Galactose – same as YPD except that glucose (glc) was replaced with 2% (w/v) galactose (gal) (Fisher Scientific); YPGly – 1% (w/v) yeast extract (Liofilchem), 2% (w/v) bactopeptone (Liofilchem), 1% (w/v) ethanol and 1% (w/v) glycerol); YPC – Yeast Peptone Combo – 1% (w/v) yeast extract (Liofilchem), 2% (w/v) bactopeptone (Liofilchem), 1.5% (w/v) galactose (Fisher Scientific), and 0.5% (w/v) glucose (Liofilchem); or Synthetic Complete drop-out medium [SC- 2% (w/v) glucose (Liofilchem)], 0.67% (w/v) yeast nitrogen base without amino acids (BD BioSciences) and supplemented with appropriate amino acids/nucleotides, depending on the strain, namely 0.008% (w/v) histidine (Sigma Aldrich), 0.008% (w/v) tryptophan (Sigma Aldrich), 0.04% (w/v) leucine (Sigma Aldrich) and 0.008% (w/v) uracil (Sigma Aldrich); SCGal – same as SC except that glucose (Liofilchem) was replaced with 2% (w/v) galactose (Liofilchem)] or minimal medium [MM - 2% (w/v) glucose (Liofilchem), 0.67% (w/v) yeast nitrogen base without amino acids (BD BioSciences) supplemented with the appropriate amino acids and nucleotides, namely 0.008% (w/v) histidine (Sigma Aldrich), 0.04% (w/v) leucine (Sigma Aldrich), 0.008% (w/v) uracil (Sigma Aldrich), 0.008% (w/v) adenine (Sigma Aldrich) and 0.008% tryptophan (Sigma Aldrich)]. For solid medium, 2% (w/v) agar (Liofilchem) was added.

Plasmid DNA was extracted using a NZY Miniprep kit (NZYtech genes & enzymes), following the manufacturer's instructions. DNA was quantified using Nanodrop 1000 (ThermoFisher Scientific).

2.4. Inducing Protein Expression - Growth Conditions

As illustrated in Table 1, different promoters were used to control kinase expression. According to each mutant's characteristics, distinct conditions were used to induce protein expression.

Cells with candidate kinases under the regulation of the *MET25* promoter (and wild type (wt)) were grown overnight in YPGal supplemented with 2mM L-Met (excess of methionine – repressing conditions) and harvested (t=0). The remaining cells were washed, transferred to SCGal supplemented with 0.05mM L-Met (low concentration of methionine - inducing conditions) and grown for 30 minutes (t=30).

Cells with Cdc28p under the regulation of a temperature-sensitive (ts) degron (and wild type) were grown overnight in YPGal at 26 °C on an orbital shaker at 140 rpm. Cells were transferred to an incubator at 37 °C (restrictive temperature – repressing conditions) on an orbital shaker at 140 rpm, for three hours to guarantee protein degradation, and harvested (t=0). The remaining cells were transferred to an incubator at 26 °C (permissive temperature – inducing conditions), grown for two hours and harvested (t=2).

Cells expressing Cdc5p under the regulation of *GAL1* promoter – p*GAL1*-Cdc5 – and wild type were grown overnight in YPC, to a OD_{600} of approximately 0.5, and 10mL of cells were harvested (t=0). The remaining cells were washed, transferred to YPGal (overexpression) and to YP+1%Gal+1%Glc (repression). After 30 minutes, 10mL of cells were collected (t=30) for each condition.

The strains Atp2-wt, Atp2-Thr124A, Atp2-Thr317A and Atp2-Thr124A/Thr317A were grown overnight in YPGal and collected when OD_{600} was approximately 0.5.

For all strains, 10 mL of cells were collected at OD_{600}= 0.5 by centrifugation at 4200 rpm for 2-4 min, pellets were washed with 500µL of 20% (w/v) trichloroacetic acid (TCA) and preserved at -80 °C until further use.

2.5. Western Blotting Analysis

Cell lysates were prepared from pellets by adding zirconia beads and 50-60µL of Laemmli sample buffer 2X without 2-mercaptoethanol (4% (w/v) SDS, 20% (v/v) glycerol, 0.004% (w/v) bromophenol blue and 0.125M Tris HCl, pH 6.8) complemented with phosphatase inhibitors (0.5M PMSF, 50 mM sodium fluoride, 5 mM sodium pyrophosphate, 1 mM sodium orthovanadate and protease inhibitors cocktail (Roche Diagnostics)). TCA remains were neutralized by addition of small volumes of 2M NaOH. Protein extraction was achieved by vigorous vortexing, in the presence of zirconia beads, for approximately 10-15 minutes (1-minute intervals on ice) and a 10-minute incubation period at 95 °C. Soluble protein was separated from cell debris by centrifugation at 13000 rpm for one minute. Protein was quantified using the commercial kit Pierce™ BCA Protein Assay Kit (ThermoFisher Scientifc), following the manufacturer's instructions.

Protein extracts (40μg) were prepared in Laemmli sample buffer 1X with 5% (v/v) 2-mercaptoethanol and heated at 95 °C for five minutes. Afterwards, protein extracts were separated by SDS-PAGE using a 10% polyacrylamide gel at 70-90V and transferred to nitrocellulose membranes using a semi-dry transfer system (20% (v/v) methanol) at 80mA/cm^2 for one hour. Protein separation and transfer was attested by Ponceau S staining (0.5% (w/v) Ponceau S, 5% (v/v) acetic acid), and after removed by Tris-buffered saline (TBS) washings before proceeding.

Each membrane was blocked with 5% (w/v) nonfat dry milk in TBS with 0.05% (vol/vol) Tween-20 (TTBS) (20 mM Tris, 140 mM NaCl, 0.05% (v/v) Tween-20, pH 7.6) for one hour. Next, membranes were incubated overnight, at 4 °C, with primary antibodies: rabbit anti-HA (Santa Cruz Biotechnology, 1:1000) or mouse anti-Cdc28 (Santa Cruz Biotechnology, 1:300). After three 5-minute washes with TTBS, membranes were probed with secondary antibodies, namely anti-rabbit IgG (Sigma, 1:7000) and anti-mouse IgG (1:6000, Molecular probes), at room temperature for 1-2 hours, followed by three 5-minute washes with TTBS and a 1-minute wash with TBS. Immunodetection was achieved by chemiluminescence using WesternBright™ ECL detection kit (Advansta), followed by exposure of membranes to LucentBlue X-ray films (Advansta).

After washing with TTBS, membranes were stripped by incubating in Stripping Buffer (62.5 mM Tris-HCl pH 6.8, 2% (w/v) SDS, 10mM 2-mercaptoethanol) for 30 minutes in a water bath at 50 °C. After complete removal of 2-mercaptoethanol, accomplished by several washes, membranes were blocked as before and re-probed overnight, at 4 °C, using rabbit anti-Atp2 (Abcam, 1:2000) or for one hour, at room temperature, using mouse anti-Pgk1 (ThermoFisher Scientific, 1:10000). Secondary antibodies were the same as before.

The intensity of the resulting bands was quantified by densitometry using Quantity One 1-D Analysis Software (Bio-Rad).

2.6. Phos-tag™ Acrylamide Analysis

To evaluate Atp2p phosphorylation levels upon manipulation of kinase expression, protein extracts were separated using a novel type of phosphate-affinity SDS-PAGE: Zn^{2+}Phos-Tag™ SDS-PAGE method.

Protein extracts (40µg – preparation as described before) were separated using a 50µM Zn^{2+}Phos-tag™ gel (Wako Pure Chemical), consisting of a separating gel (6% (v/v) polyacrylamide and 357mM Bis-Tris-HCl, pH 6.8) and a stacking gel (4% (v/v) polyacrylamide and 357mM Bis-Tris-HCl, pH 6.8). The running buffer was composed of 0.10M Tris, 0.10M MOPS, 5mM sodium bisulfite and 0.10% (w/v) SDS, pH 7.8. Protein electrophoresis was carried out at 55V since low voltage improves the protein resolution for this method. Before transfer to nitrocellulose membranes, gels were washed three times, 10 minutes each, with semi-dry transfer buffer lacking methanol (25mM Tris, 192mM glycine) complemented with 10mM EDTA. The gel was also additionally washed for 10 minutes in transfer buffer with 10% (v/v) methanol – also used for protein transfer to a nitrocellulose membrane, at 100mA/cm^2, for one hour. Protein transfer was evaluated by Ponceau S staining, followed by a blocking step using 5% (w/v) nonfat dry milk in TTBS, for one hour. Afterwards, membranes were incubated with a primary antibody against Atp2 (Abcam, 1:2000) overnight at 4 °C. The remaining procedure was performed as described above for Western Blotting analysis.

2.6.1. Alkaline Phosphatase Treatment

As a control for Atp2 phosphorylation detection, wild type cells were treated with alkaline phosphatase. Cells were grown overnight in YPGal and harvested. Cell lysis was achieved using 50µL of 50mM sodium potassium phosphate buffer (pH 7.0) by vigorous vortexing in the presence of zirconia beads for 15 minutes (1-minute intervals on ice). Soluble protein was separated from cell debris by centrifugation at 13000 rpm for one minute. Protein was quantified using the commercial kit Pierce™ BCA Protein Assay Kit (ThermoFisher Scientific) following the manufacturer's instructions.

Treatment consisted of an incubation period of two hours, at 37 °C, in an orbital shaker at 140 rpm of the following reaction mix: 40µg of protein, 2µL of a 100X stock solution of Protease Inhibitors cocktail (Roche Diagnostics), 20 U/µL of 1X FastAP reaction buffer (ThermoFisher Scientific), 50 U/µL of FastAP Thermosensitive Alkaline Phosphatase (ThermoFisher Scientific) and the adequate amount of autoclaved water for a final volume of 200µL. The control sample was treated with water instead of the alkaline phosphatase. Subsequently, 200µL of 20% TCA was added and the mixture was kept on ice for 15 minutes before being centrifuged at 13000 rpm, at 4 °C, for approximately 20 minutes. After removal of the supernatant, the treated protein was dissolved in 12µL of Laemmli sample buffer 2X, incubated at 95 °C for five minutes and separated using a Zn^{2+}Phos-Tag™ SDS-PAGE gel, as described previously.

2.7. Oxygen Consumption Rate Measurements

The oxygen consumption rate (OCR) was measured with a Clark electrode. Cells were grown to OD_{600}=1 in liquid media with varying percentages of galactose and glucose, 3 x 10^8 whole cells were collected by centrifugation, resuspended in 1mL of phosphate buffer (137 mM NaCl pH 7.4, 2.7 mM KCl, 8 mM Na_2HPO_4 and 1.46 mM KH_2PO_4), and transferred to a microcell, magnetically stirred, at room temperature. The OCR was measured for two minutes using an OXYgraph (Hansatech) oxygen electrode system and the resulting data was analyzed using the software Oxy32 v2.25.

2.8. Respiratory Growth Capacity

To evaluate respiratory growth capacity, yeast cells were grown in plates containing strict respiratory carbon source, glycerol (VWR Chemicals). The strains BY4741, p*MET25*-Pkc1, p*MET25*-Ipl1, p*MET25*-Ccd5 and p*MET25*-Hrr25 were grown overnight in YPD at 26 °C. Each culture was diluted to OD_{600}=0.1 and ten-fold dilutions were performed using phosphate buffer. For each strain and dilution, 7µL of cells were spotted in YPD and YPGly and incubated at 26 °C, for 2-3 days. Three independent assays were performed for each strain.

2.9. Specific Growth Rate and Ten-fold Dilution Series

To determine the specific growth rate, cells of the p*GAL1*-Cdc5, Δ*atp2* p*GAL1*-Cdc5, Δ*atp2* p*GAL1*-Cdc5 [pRS316-ATP2] and Δ*atp2* p*GAL1*-Cdc5 [pRS316-ATP2-Thr124A/Thr317A] strains were grown overnight in selective media, at 26 °C. In the morning, OD_{600} was measured and cells from each strain were inoculated in YPGal (starting OD_{600}=0.1). Growth was monitored over a period of 10 hours via OD_{600} measurements and plotted as a function of time. The specific growth rate corresponds to the slope of each calculated growth curve.

Ten-fold dilution series of cells from these strains, as well as BY4741 and *Δatp2*, were also performed. After overnight growth in selective media, each culture was diluted to OD_{600}=0.1 and ten-fold dilutions were performed using phosphate buffer. For each strain and dilution, 7µL of cells were spotted and incubated at 26 °C, for 2-3 days, in plates with four different compositions: YPD, YPGal, YPC and YP+1%Gal+1%Glc. Three independent assays were performed for each strain.

2.10. Statistical Analysis

All statistical analysis were performed using GraphPad Prism v8.0.2 Software. Values were compared by one-way ANOVA or two-way ANOVA with Tukey's multiple comparisons, respectively. Fisher's exact test against control was also used.

3. Results and Discussion

3.1. *In silico* Prediction of Atp2$^{Thr124/Thr317}$ Kinase Regulators

Bioinformatics tools were used for the prediction of kinase regulators of the Atp2$^{Thr124/Thr317}$ phosphosites. The chosen software, GPS: Group-based prediction system 3.0, uses the consensus sequence that integrates each of the phosphosites of interest with the goal of identifying kinases that share a similar consensus motif. This software has proven to predict more than 13000 phosphorylation sites and its regulatory kinases with high precision (Xue *et al.*, 2008); however, likewise all the available informatic predictors, this software was designed for mammalian kinase motifs. Nevertheless, considering that there is high conservation of phosphorylation motifs for homologous yeast kinases (about half is conserved) (McDonald, Trost and Napper, 2018) , there is a high chance to predict the correct yeast kinase using this software.

The resulting data for each search contains different information, such as the kinase, score and cutoff, as demonstrated in Figure 5. The score is an algorithm-calculated value that assesses the potential of phosphorylation, and therefore higher score values equals higher likelihood of the residue being phosphorylated by the respective kinase.

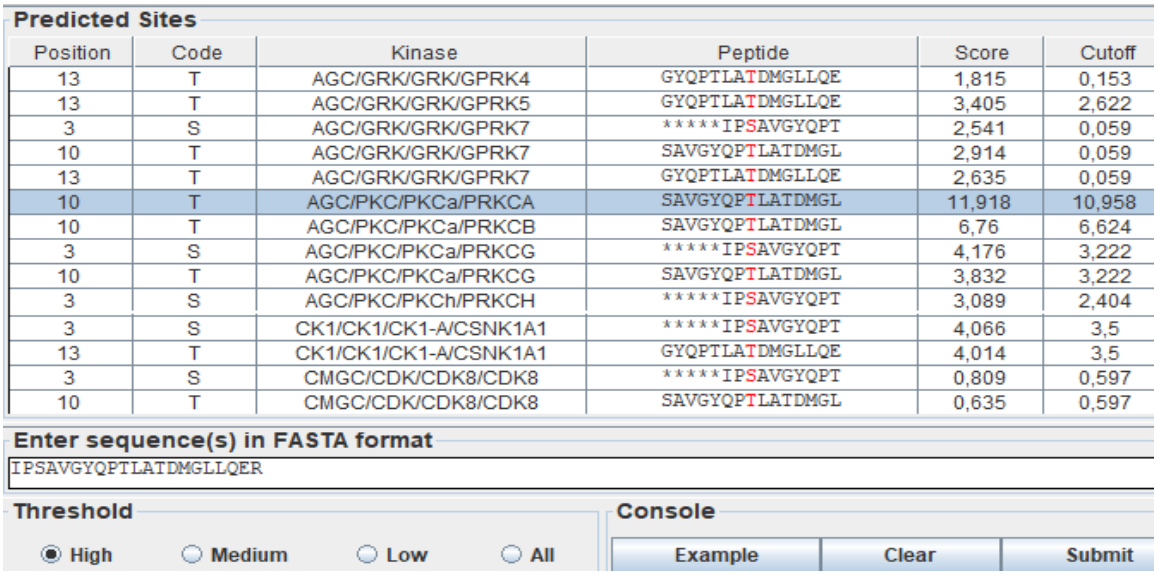

Predicted Sites

Position	Code	Kinase	Peptide	Score	Cutoff
13	T	AGC/GRK/GRK/GPRK4	GYQPTLATDMGLLQE	1,815	0,153
13	T	AGC/GRK/GRK/GPRK5	GYQPTLATDMGLLQE	3,405	2,622
3	S	AGC/GRK/GRK/GPRK7	*****IPSAVGYQPT	2,541	0,059
10	T	AGC/GRK/GRK/GPRK7	SAVGYQPTLATDMGL	2,914	0,059
13	T	AGC/GRK/GRK/GPRK7	GYQPTLATDMGLLQE	2,635	0,059
10	T	AGC/PKC/PKCa/PRKCA	SAVGYQPTLATDMGL	11,918	10,958
10	T	AGC/PKC/PKCa/PRKCB	SAVGYQPTLATDMGL	6,76	6,624
3	S	AGC/PKC/PKCa/PRKCG	*****IPSAVGYQPT	4,176	3,222
10	T	AGC/PKC/PKCa/PRKCG	SAVGYQPTLATDMGL	3,832	3,222
3	S	AGC/PKC/PKCh/PRKCH	*****IPSAVGYQPT	3,089	2,404
3	S	CK1/CK1/CK1-A/CSNK1A1	*****IPSAVGYQPT	4,066	3,5
13	T	CK1/CK1/CK1-A/CSNK1A1	GYQPTLATDMGLLQE	4,014	3,5
3	S	CMGC/CDK/CDK8/CDK8	*****IPSAVGYQPT	0,809	0,597
10	T	CMGC/CDK/CDK8/CDK8	SAVGYQPTLATDMGL	0,635	0,597

Enter sequence(s) in FASTA format

IPSAVGYQPTLATDMGLLQER

Threshold

High Medium Low All

Console

Example Clear Submit

Figure 5 - Representation of kinase search using GPS 3.0. The used sequence in this example refers to the phosphosite Atp2^{Thr317}.

Using the previously identified sequences that integrate the phosphosites of interest, Thr124 and Thr317, and using the higher threshold, corresponding to the lowest theoretical maximal false positive rate, 61 kinases were predicted to potentially regulate these sites, that is approximately half of all existent kinases in *S. cerevisiae* (±130 kinases) (Ohlmeier, Hiltunen and Bergmann, 2010). From those, four kinases, whose closest homologs in yeast are Ipl1, Pkc1, Hrr25 and Cdc5, stood out with the highest score values, and were therefore selected (Table 3). Curiously, two kinases, Hrr25 and Pkc1, registered high score values for both Atp2p phosphosites.

Table 3 – Predicted kinases and score values for each Atp2p phosphosite, and respective yeast homologs.

	MAMMALIAN KINASE	SCORE	HOMOLOG YEAST KINASE
T124	Ipl1/AUR	8.111	Ipl1
T124 / T317	Pkc	8.253 / 11.918	Pkc1
T124 / T317	Vrk2	23.25 / 14.5	Hrr25
T124	Plk	10.688	Cdc5

Ipl1 is the *S. cerevisiae* aurora kinase, an important regulator of chromosome segregation as well as the mitotic DNA integrity checkpoint (Buvelot *et al.*, 2003). Pkc1

participates in the regulation of cell growth, proliferation and progression through the cell cycle. Pkc1 is the only protein kinase C in *S. cerevisiae*, being therefore homolog to the PKC isozymes described previously. Additionally, Pkc1 kinase activity is counterbalanced by Sit4 phosphatase activity, suggesting common targets (De La Torre-Ruiz *et al.*, 2002).

Hrr25p is a conserved casein kinase that participates in vesicular traffic, DNA repair and protein synthesis. Hrr25 also shares substrates with the phosphatase Sit4 (Mehlgarten *et al.*, 2009). Cdc5p is a polo-like kinase, conserved from yeast to humans. Cdc5p is an important cell cycle regulator, participating in events from S-phase to cytokinesis (Simpson-Lavy and Brandeis, 2011). Interestingly, this kinase has been reported as essential for mtDNA transmission, suggesting a role in mitochondrial function (Dutcher, 1982; García-Rodríguez *et al.*, 2009).

Since Hrr25 and Pkc1, the kinases that registered high score values for both phosphosites, have been reported to share substrates with Sit4, the phosphatase that has been described as a regulator of Atp2, we postulated that they may be involved in the phosphoregulation of Atp2p.

3.2. Establishment of Zn^{2+}Phos-Tag™ SDS-PAGE

Since the main goal of this project was to identify regulatory kinases of the $Atp2^{Thr124/Thr317}$ residues, detection of Atp2p phosphorylation was crucial. In recent years, different methods to study protein phosphorylation have been developed and some of them have been applied to the study of Atp2p, as aforementioned. In this study, the chosen technique was a Phos-Tag™ gel retardation assay.

Briefly, this novel procedure is an electrophoresis technique capable of separating phosphorylated and non-phosphorylated forms of a protein. In the presence of zinc or manganese ions, the Phos-Tag™ functional molecule binds to phosphorylated residues, resulting in differentiated migration velocities and consequent separation of proteins according to their phosphorylation status (Kinoshita and Kinoshita-Kikuta, 2011). Currently, two different versions exist, Mn^{2+} and Zn^{2+}Phos-Tag™, with different buffer compositions and resolving capabilities. Since the zinc option has improved detection of shifts in protein mobility, when compared to its Mn^{2+} counterpart, and the gels are stable for longer periods

after casting (Kinoshita and Kinoshita-Kikuta, 2011), it was the selected option for this project.

The implementation phase consisted in determining the appropriate concentration of acrylamide and Phos-Tag™ Acrylamide that allows the separation of the Atp2 phosphorylated forms. The manufacturer's guide recommends using 8% acrylamide gels for proteins <60kDa, such as Atp2 (55 kDa), however, better results were obtained using 6% acrylamide gels.

More than one phosphorylation band was expected as in addition to the two phosphoresidues, Thr124 and Thr317, other phosphorylation sites have been described for this protein (Figure 3). Though for some proteins several phosphorylated bands are observed when using Phos-Tag™, for others, which seems to be the case for Atp2, there is a single band shift that may contain several phosphorylated residues. Another hypothesis is that one single phosphosite is highly abundant, and the others are under the detection limit. Additionally, even when testing different Phos-Tag™ concentrations only one single band for Atp2 was observed. The molecular weight of that single band is decreased, comparatively to the wild type, after treatment with alkaline phosphatase to dephosphorylate the protein (Figure 6A). Different Phos-Tag™ concentrations were also tested and 50μM Phos-Tag™ Acrylamide resulted in the greatest separation capacity for the protein of interest.

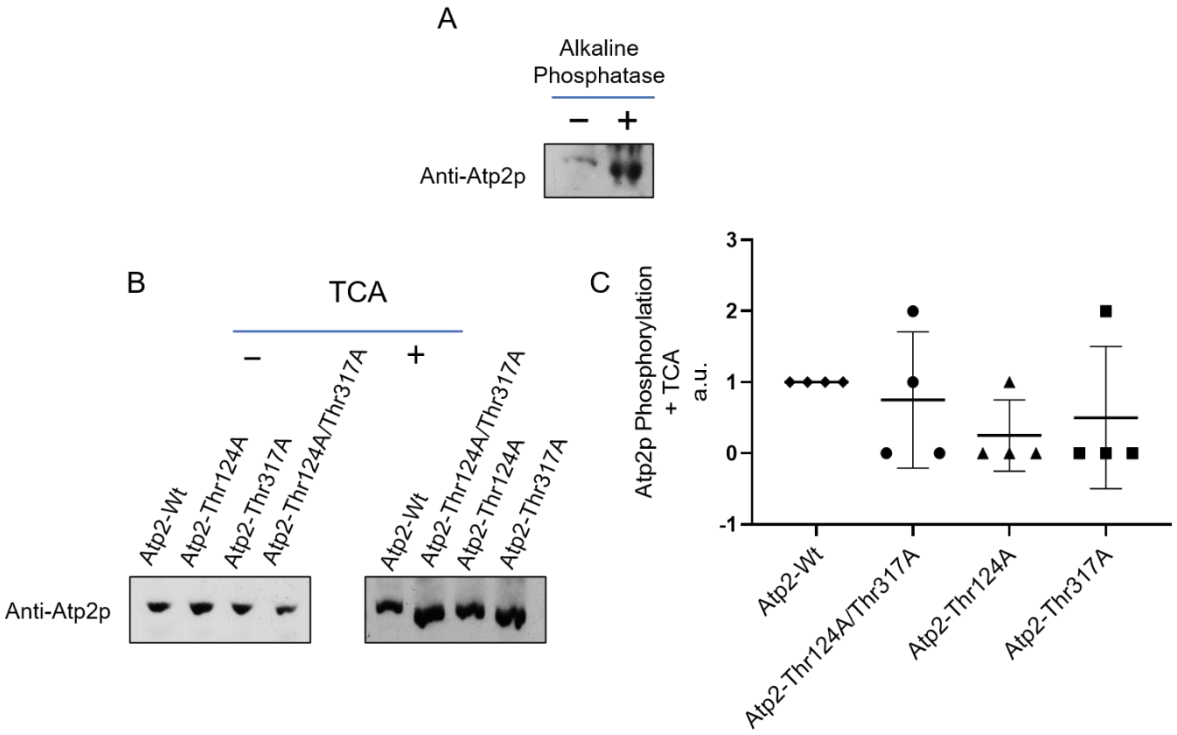

Figure 6 - Immunodetection of Atp2p following Phos-Tag™ SDS-PAGE. A. Phos-Tag™ SDS-PAGE analysis of the wild type treated with (+) and without (-) alkaline phosphatase (n=3). B. Phos-Tag™ SDS-PAGE analysis of the strains Atp2-wt, Atp2-Thr124A, Atp2-Thr317A and Atp2-Thr124A/Thr317A with (+) and without (-) TCA treatment. C. Graphical representation of the band shifts obtained for the assays performed for the strains Atp2-Wt, Atp2-Thr124A, Atp2-Thr317A and Atp2-Thr124A/Thr317A (n=4). Each phosphorylation band was given a number according to its relative position compared to the wild type (0 for lower, 1 for equal and 2 when higher). These scores are used throughout the study.

To assess if this method is suitable to detect phosphorylation at the residues Thr124/Thr317, the phosphorylation status upon expression of Atp2 with the identified residues mutated into the phosphoresistant alanine was evaluated. Phosphoresistant mutants, Atp2-Thr124A, Atp2-Thr317A and Atp2-Thr124A/Thr317A, as well as Atp2-wt (control), were expressed from a plasmid under the regulation of its own promoter, in cells lacking the endogenous Atp2 (Pereira *et al.*, 2018). Since Thr124A/Thr317A mutations prevent phosphorylation at these residues, a down-shifted band corresponding to less Atp2p phosphorylation was expected comparatively to the cells expressing the wild type Atp2. Cells were grown, analyzed in a Phos-Tag™ SDS-PAGE and results are shown in Figure 6B. The first assay was inconclusive since there was no noticeable shift for any strain, relatively to the wild type, most likely due to protein dephosphorylation between collection and analysis. So, to avoid protein degradation and dephosphorylation, sample preparation

was improved by adding a TCA incubation step, which arrests cells metabolism, preserving the phosphorylated state of the proteins. Cells treated with TCA were evaluated and the results, shown in Figure 6B, are in agreement with expectations, showing lowered phosphorylation bands for all phosphoresistant mutants, relatively to the wild type. Furthermore, the difference in results between samples treated with or without TCA (Figure 6B) is evident, highlighting the importance of the preservation step during sample preparation.

In Figure 6C, the phosphorylation status for the replicas performed for the phosphoresistant mutants, when compared to the wild type, is shown. By observing the mean, represented in the graph as a horizontal line, we can see that the tendency for all three strains is to have phosphorylation bands lower than the phosphorylation band present in the wild type, which indicates dephosphorylation, as anticipated.

Together, these results validate the use of the Phos-Tag™ SDS-PAGE method for the purposes of this study, detection of Atp2 phosphorylation.

3.3. Experimental Evaluation of the Atp2$^{Thr124/Thr317}$ Predicted Kinase Regulators

To determine if the kinases selected *in silico* are phosphoregulators of Atp2p, two different approaches were used: assessment of the phosphorylation state of Atp2p and evaluation of the Atp2p levels upon manipulation of kinase expression. Atp2 levels provide an indirect evidence of Atp2 phosphorylation since it was reported that increased phosphorylation of Atp2p$^{Thr124/Thr317}$ is accompanied by higher protein levels probably due to stabilization of the protein (Pereira *et al.*, 2018).

In addition to the four *in silico* predicted kinases, the kinase Cdc28 was also evaluated as a potential Atp2p regulator, since in previous work from the group a genetic interaction was observed, suggesting the two proteins are functionally related (Pereira et al., 2018; Unpublished). Cdc28 is a cyclin-dependent kinase, homolog to the human Cdk1 – cyclin-dependent kinase 1. This kinase is the central coordinator of the mitotic cell cycle in budding yeast, associating alternately with G1, S and G2/M phase cyclins (Mendenhall and Hodge, 1998).

3.3.1. Regulating Kinase Expression

The premise of this study is that in the absence of a potential Atp2p phosphoregulator, Atp2p phosphorylation should decrease due to loss of kinase-mediated phosphorylation and upon kinase overexpression, Atp2p phosphorylation should increase. Since all the selected kinases are encoded by essential genes in the BY4741 strain, regulatable promoters were used to achieve both kinase repression and overexpression.

For most kinases, the heterologous promoter *MET25* was introduced (Figure 7) in the genome to replace the endogenous kinase promoter, allowing regulation of kinase expression by manipulation of external factors. *MET25* is an inducible promoter that represses transcriptional expression in the presence of methionine. These kinases were also tagged with three copies of hemagglutinin, 3HA (Figure 7), to allow monitoring of protein expression since no commercial antibodies are available. To study *CDC28*, however, a temperature-sensitive mutant was used since it was already available in the laboratory collection.

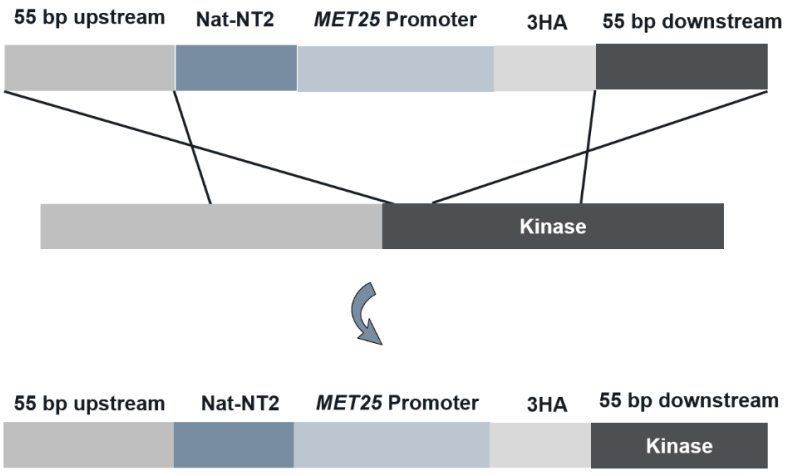

Figure 7 - Schematic representation of the N-terminal fusion cassette used to construct strains expressed under regulation of p*MET25*. Integration of the cassette into the yeast genome was accomplished by homologous recombination.

Initially, an overnight repression was used for the kinases under the regulation of the inducible promoter: Cdc5p, Hrr25p, Ipl1p and Pkc1p. Cells were evaluated during log phase in which kinases tend to be more active, since signaling pathways are also more active during

exponential growth. However, Atp2p levels are usually low in this phase when the carbon source is glucose since mitochondria are repressed during fermentation. For this reason, cells were grown in semi-respiratory conditions, using galactose as a carbon source, leading to increased levels of Atp2p and consequent facilitation of its detection. In addition, media contained excess L-methionine to inhibit kinase expression, mediated by p*MET25*.

MET25 promoter has been shown to exhibit weak expression in its repressed state (Janke *et al.*, 2004). Thus, protein expression was not completely inhibited, allowing growth of the mutant strains, albeit more slowly. This prolonged repression seemed to decrease kinase levels for every strain except for p*MET25*-Hrr25 which showed no signs of repression (Figure 8). Figure 8 also illustrates the appearance of 2 closely located bands for the p*MET25*-Hrr25 strain when probed with anti-HA (see Figure S1), which likely reflects protein degradation.

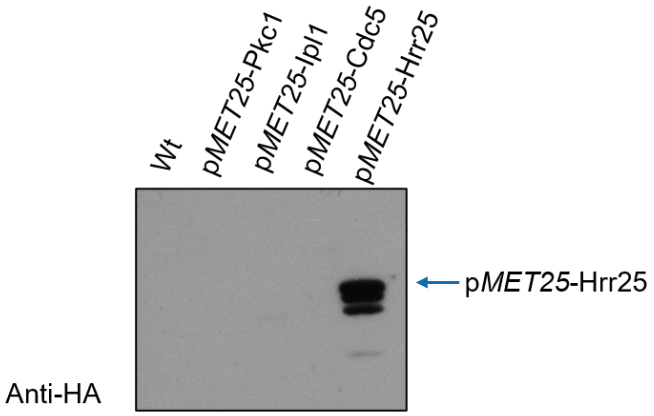

Figure 8 - Western Blot analysis of the constructs carrying the kinases under regulation of the *MET25* promoter, probed with anti-HA to evaluate protein expression, after overnight growth in repressing conditions.

In addition to kinase repression, which may decrease Atp2p phosphorylation, kinase overexpression, which may lead to an increase in Atp2p phosphorylation, was also tested. For this approach, an overnight repression followed by a brief period of protein overexpression, induced by minimal methionine concentration, was evaluated.

Firstly, it was determined the time needed for kinase expression to resume, after the overnight growth in repressing conditions. To do so, cells were switched to inducing conditions and different time points were evaluated. Results show that 30 minutes is sufficient for recovery of protein expression (see Figure S2). The increase in kinase expression between the repressed (t=0) and overexpressed states (t=30), observed when

probed with anti-HA, is evident for all the kinases (Figure 9A). p*MET25*-Hrr25 was not tested, as expression was identical in repression and overexpression conditions. In Figure 9A, it is also possible to observe a low protein expression under regulation of p*MET25*, even in the repressed state (t=0), which may sustain strain growth in these conditions, as mentioned before.

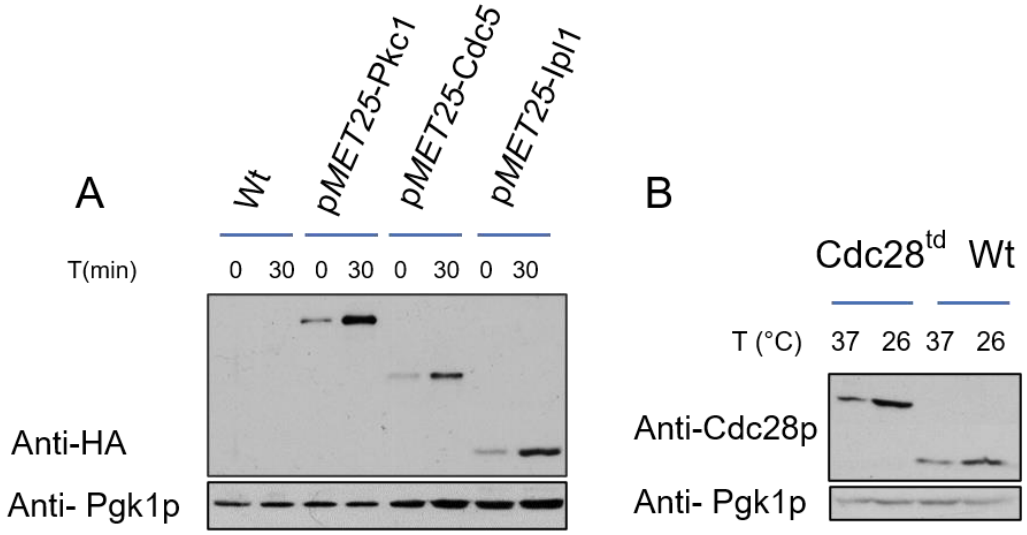

Figure 9 – Western blot analysis of kinase expression. A. Analysis of the constructs carrying the *MET25* promoter, probed with anti-HA to evaluate protein expression. Cells were collected after overnight growth in repressing conditions (t=0) and after a 30-minute incubation period in inducing conditions (t=30). B. Analysis of protein expression for the strain Cdc28^{td}, probed with anti-Cdc28p to evaluate protein expression. Cells were incubated at the non-permissive temperature (37 °C) for three hours and shifted to the permissive temperature (26 °C) for two hours. Pgk1p is shown as a loading control.

Since this strategy was not effective for p*MET25*-Hrr25, different repressing conditions were tested but none of these newly tested conditions were effective at inhibiting Hrr25p expression (see Figure S1), meaning this approach was not viable for the study of *HRR25*. Hence, a different strategy was tested to regulate Hrr25p expression.

Kafadar *et al*. described the use of an unstable protein module – a degron – fused to the N-terminal of HA-Hrr25 and expressed from a plasmid, which was then expressed under regulation of a galactose promoter (Kafadar *et al.*, 2003). Using this construct, Hrr25 expression is normal when the carbon source is galactose, however, this unstable degron causes rapid termination of protein expression and subsequent degradation upon addition of glucose.

This approach was thus tested, using the plasmid expressing the described module kindly provided by the authors. Cells were grown in glucose as a carbon source, conditions

that cause protein degradation, and switched to galactose as a carbon source, conditions that allow protein stability. However, cells exhibited unstable Hrr25p expression even in galactose conditions, making it unsuitable to be used (data not shown).

Replacement of the Hrr25 promoter with another regulatable promoter, the *GAL1* promoter (likewise for p*MET25*) was also attempted, but no viable transformants were obtained.

To study the Cdc28 kinase a temperature-sensitive mutant was employed, whose permissive temperature is 23 °C and whose restrictive temperature is 37°C, at which protein unfolds and the fused N-degron causes protein degradation. The regulation of protein expression for this strain was similar to the one used for the *MET25* promoter: cells were grown in repressive conditions (37 °C) and switched to inducing conditions (26 °C), resulting in expression of the kinase.

Hence, the first step consisted in assessing the time needed for cells to recover protein expression after the protein degradation period at the non-permissive temperature. Analysis of the time points evaluated show that after growth in non-permissive conditions, two hours are necessary, at the permissive temperature, to obtain a clear increase in Cdc28p levels (see Figure S3). Recovery of protein expression is shown Figure 9B, detected by probing with anti-Cdc28p, when cells were switched from 37 °C to 26 °C. The increase in molecular weight in the band corresponding to the $Cdc28^{td}$ strain is reflective of the fusion of the N-degron. Figure 9B also shows levels of native Cdc28 detected in the wild type, with a smaller molecular weight, when probed with anti-Cdc28p.

3.3.2. Evaluation of Atp2p Phosphorylation upon Kinase Repression/Overexpression

After determining the conditions for regulation of kinase expression, the effect of repressing/overexpressing the selected kinases in the phosphorylation status of Atp2p was evaluated, using the Zn^{2+}Phos-tag™ SDS-PAGE assay.

When using repressing conditions, the Atp2p band was expected to be lower than the wild type band if the repressed kinase is required for Atp2p phosphorylation. Figure 10 shows the phosphorylation bands relative to overnight repression assays, in which cells

expressing the kinases under regulation of *MET25* promoter were grown in excessive concentration of L-methionine, to repress kinase expression. The up-shift in phosphorylation bands between p*MET25*-Pkc1 and wt, for instance, is clear. For each independent assay, a score was attributed to each phosphorylation band of interest, based on its position relative to its control band, in this case the wt band. We observed that, unlike expected, kinase repression causes no effect, or induces Atp2p phosphorylation, in these growth conditions (Figure 10). For Pkc1p and Hrr25p the increase in phosphorylation is more pronounced than for the other strains. These unforeseen results may be explained by the fact that *MET25* is not a completely repressive promoter, and since kinase expression levels are usually low, the repression obtained may not be efficient. This is even more likely for Hrr25 since high expression was always observed. Since we have not compared kinase expression upon *MET25* repression with physiological kinase expression, we cannot be certain that kinase repression was achieved. Another explanation for the increase in phosphorylation upon kinase repression may be due to indirect effects of the kinases in Atp2 phosphorylation.

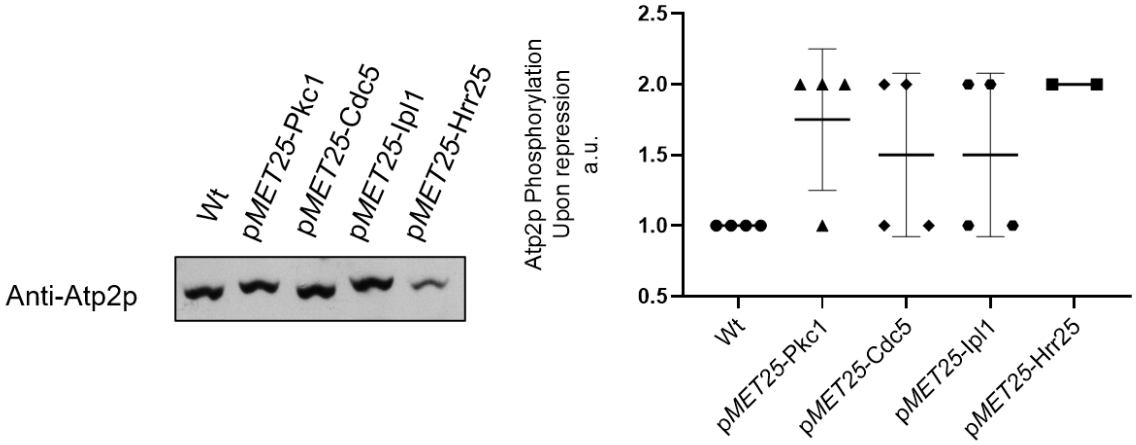

Figure 10 – Phos-Tag™ SDS-PAGE analysis of phosphorylation status of Atp2p for repressed kinases. Representative immunoblot and graphical representation of phosphorylation of Atp2p in p*MET25* regulated kinases, after overnight growth in repressing conditions. Each phosphorylation band was given a number according to its relative position compared to the wild type.

The effects of overexpressing hit kinases in Atp2p phosphorylation were also evaluated and are depicted in Figure 11A. In this case, since we are comparing two conditions with low and high kinase expression (Figure 9), the kinase endogenous levels are irrelevant. Cells overexpressing the 3 kinases, Pkc1, Cdc5 and Ipl1, exhibit a tendency to increase Atp2p phosphorylation relatively to wt, but particularly Cdc5. Curiously, the shift

from repressive to inductive media tended to cause a dephosphorylation of Atp2p in wild type (Figure 11A).

Cdc28 ts mutant cells, that contain a degron fusion, are expected to be functionally unperturbed at permissive temperature (Dohmen, Wu and Varshavsky, 1994), meaning that expression levels of protein should be unaltered relatively to wild type Cdc28p. Therefore, in this study, phosphorylation bands at the non-permissive temperature, 37 °C, (repressed state) were compared to the phosphorylation bands present for the permissive temperature, 26 °C (Figure 11B). A graphical representation of the replicas is also shown (Figure 11B). Evaluation of the results reveals that in the absence of Cdc28 no dephosphorylation of Atp2p occurred, indicating Cdc28 does not seem to regulate Atp2p phosphorylation.

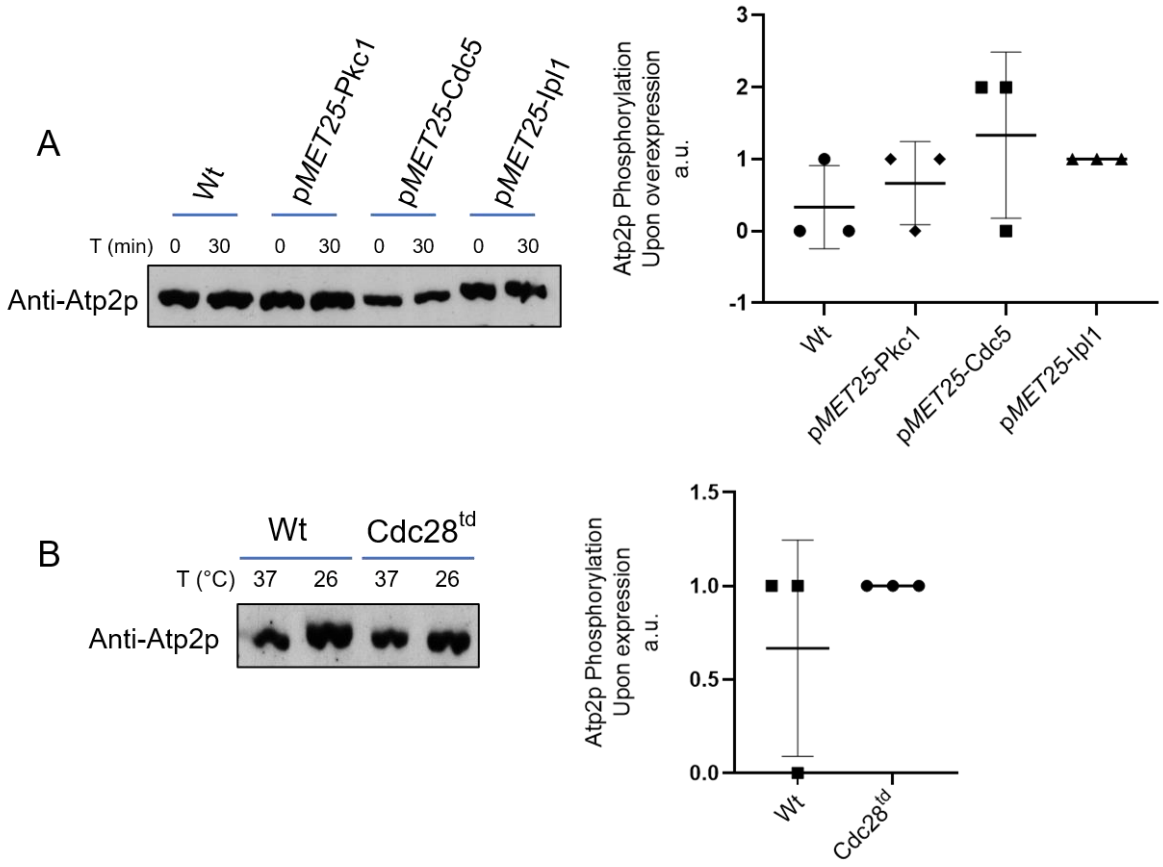

Figure 11 – Phos-Tag™ SDS-PAGE analysis of phosphorylation status of Atp2p. A. Representative immunoblot and graphical representation of phosphorylation of Atp2p in p*MET25* regulated kinases, in overexpressing conditions (30 min). Each phosphorylation band was given a number according to its relative position compared to its repressed state (t=0). B. Representative immunoblot and graphical representation of phosphorylation of Atp2p in Cdc28^{td} and wild type, in reduced Cdc28 levels (non-permissive – 37 °C) and normal Cdc28 levels (permissive – 26 °C). Each phosphorylation band was given a number according to its relative position compared to its expressed state (26 °C).

Overall, from these assays, it was possible to observe that while overexpressing Cdc5, Ipl1 and Pkc1 results in increased Atp2p phosphorylation, the same is not verified for Cdc28. Since we cannot be confident that the *MET25* repression conditions are in fact decreasing the kinase levels, we selected the most promising kinases from the Phos-Tag™ assays based on the overexpression assays. From these, Cdc5 seems to be the most promising kinase for the regulation of Atp2p. Regarding Hrr25p, since its expression could not be properly regulated, we cannot conclude on the role of Hrr25 on Atp2p regulation.

3.3.3. Evaluation of Endogenous Atp2p Levels

Since Atp2p phosphorylation at Thr124/Thr317 was associated with increased Atp2p levels (Pereira *et al.*, 2018), we analyzed the Atp2p levels upon kinase repression/overexpression using the same growth conditions as before.

The first analysis, shown in Figure 12, represents the levels of Atp2p in repressing conditions. In these conditions, Atp2p levels should decrease since kinases are repressed, and therefore less available to phosphorylate Atp2p, which in turn should lead to lower Atp2p levels. Results show increased levels of Atp2p when Pkc1p is repressed, approximately 2-fold comparatively to the wild type (Figure 12), which is consistent with the phosphorylation assays in which Atp2p phosphorylation unexpectedly increased upon Pkc1p repression. Comparatively to the wild-type, results show diminished levels of endogenous Atp2p when Cdc5p and Hrr25 are repressed. Though the decrease in Atp2p levels was expected for the repressed kinases, since Atp2p phosphorylation was increased and not decreased (Figure 10), the low Atp2p levels in these strains may be unrelated to the Atp2p phosphorylation status.

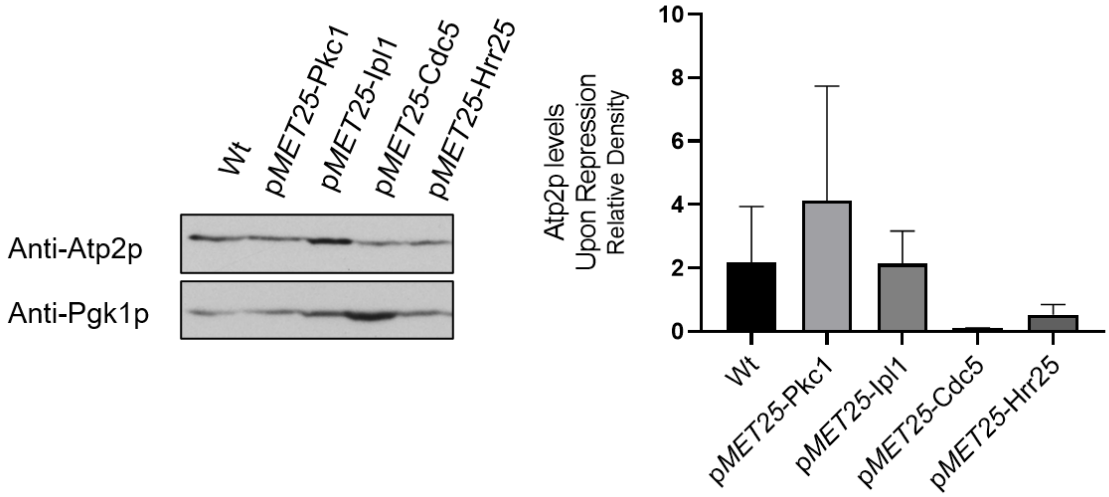

Figure 12 – Analysis of Atp2p levels for kinase repression. A. Western Blot analysis of Atp2p levels for the kinases under regulation of p*MET25*. Cells were grown overnight in repressing conditions and probed with anti-atp2p to evaluate Atp2p levels upon kinase repression. Pgk1 is shown as a loading control. B. Semi-quantitative analysis of endogenous levels of Atp2p for the strains under kinase repression (n=2). Values are the mean ± SEM, one-way ANOVA, Tukey's test. None of the strains reached statistical significance.

Atp2p levels were also evaluated for the overexpression conditions. Cells were grown in the same conditions as before and Atp2p levels were evaluated by probing with anti-atp2p, as demonstrated in Figure 13. Results demonstrate that only overexpression of Ipl1 results in increased levels of endogenous Atp2p (Figure 13), which is in agreement with the increased phosphorylation. As for Cdc5p overexpression, there is an increase in Atp2p levels, but it is minimal, as the overall Atp2 levels, as observed upon Cdc5 repression, are very low (Figure 13). Since Cdc5 was described as essential in mtDNA transmission (Dutcher, 1982) and mtDNA encodes two subunits of ATP synthase whose absence suppress the entire complex, this may explain why Atp2p levels are overall much lower for Cdc5 than for the other kinases. Overexpression of Pkc1p, on the other hand, unlike for the repression conditions, results in diminished levels of endogenous Atp2p.

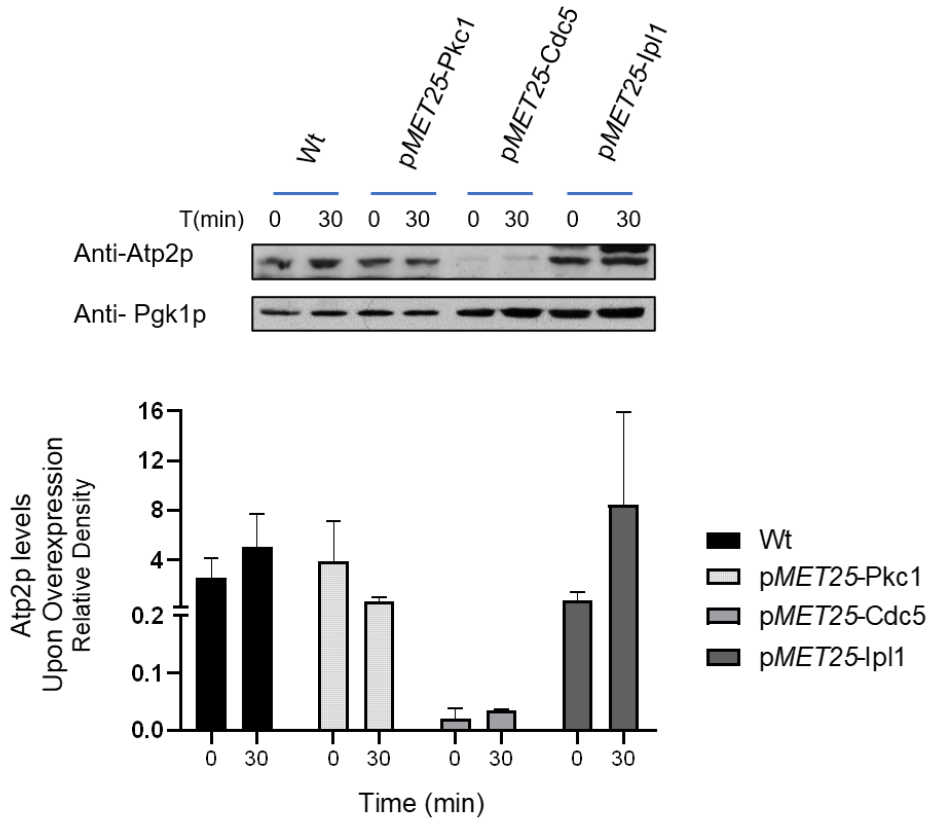

Figure 13 – Analysis of Atp2p levels for kinase overexpression. A. Western Blot analysis of the kinases under regulation of p*MET25*, probed with anti-Atp2p. Cells were collected after overnight growth in repressing conditions (t=0) and after a 30-minute incubation period in inducing conditions (t=30). B. Semi-quantitative analysis of endogenous levels of Atp2p for the same growth conditions. Sample size is n=3 for Pkc1 and n=2 for the remaining strains. Values are the mean ± SEM, two-way ANOVA, Tukey's multiple comparisons test. No statistical significance between conditions.

Lastly, the effect of expressing or repressing Cdc28p on the levels of endogenous Atp2p was also assessed (Figure 14). Cells were grown as discussed above. The results show an increase in endogenous Atp2p levels upon downregulation of Cdc28p (37 °C), comparatively to the levels obtained for the permissive temperature (Figure 14), even though no statistical difference was noted. These results are consistent with the results obtained in the Phos-Tag™ assays, in which absence of Cdc28 did not cause Atp2 dephosphorylation (Figure 11B), indicating that Cdc28 does not regulate Atp2 phosphorylation.

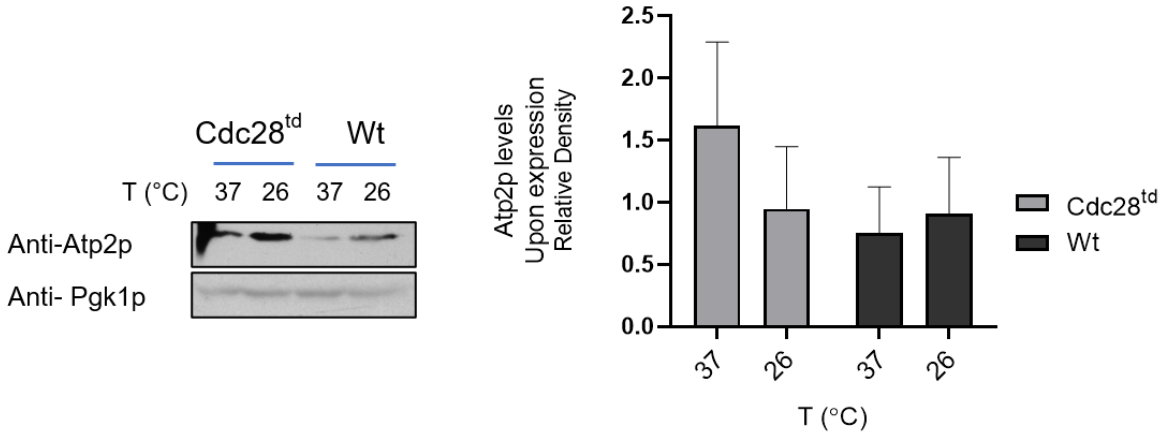

Figure 14 – Analysis of endogenous levels of Atp2p for Cdc28^{td} and wild type. A. Western Blot evaluation of protein expression for the strains Cdc28^{td} and wild type, probed with anti-Atp2p. Cells were incubated at the non-permissive temperature (37 °C) for three hours and shifted to the permissive temperature (26 °C) for two hours. Pgk1p is shown as a loading control. B. Semi-quantitative analysis of endogenous levels of Atp2p for Cdc28^{td} and wild type, in the same growth conditions. Values are the mean ± SEM n=3, two-way ANOVA, Tukey's multiple comparisons test. No statistical significance between conditions.

For the same reasons as before, we selected the most promising candidates from the overexpression assays. Overexpression of Ipl1p caused an increase in the protein levels of Atp2p. Overexpression of Cdc5p also resulted in increased Atp2p levels, although minor.

3.4. Evaluating Cdc5p as a Potential Atp2p Regulator

Considering that Cdc5 was the most promising kinase in the phosphorylation assays and that its overexpression caused an increase in Atp2 levels (even though small comparatively to the wild type), it was selected to be further evaluated as an Atp2 regulator. Since *MET25-CDC5* is not efficiently repressed, the promotor *GAL1* (p*GAL1*) was used to regulate Cdc5p expression since it is more tightly repressed than *MET25*. p*GAL1* is controlled by the available carbon source: protein expression is induced when the carbon source is galactose and inhibited when the carbon source is glucose.

First, different combinations from both carbon sources were evaluated for p*GAL1*-Cdc5 and wild type, in order to find the concentration that best approximated the growth of the mutant to the growth of the wild type, indicating wt levels of Cdc5 expression since both repression and overexpression of Cdc5 is reported to affect growth (Walters *et al.*, 2014).

These preliminary assays determined the sugar composition hereinafter used as a control, 1.5% galactose and 0.5% glucose.

Second, the simultaneous repressing and inducing capability of p*GAL1*-Cdc5 was evaluated. Cells were grown overnight in control conditions (1.5% Gal 0.5% Glc) and split in two: half culture inoculated in repressing conditions, 1% Gal 1% Glc, and the other half inoculated in inducing conditions, 2% Gal. This assay also permitted evaluation of the time needed to regulate the expression of Cdc5p in both conditions. The results are shown in Figure 15.

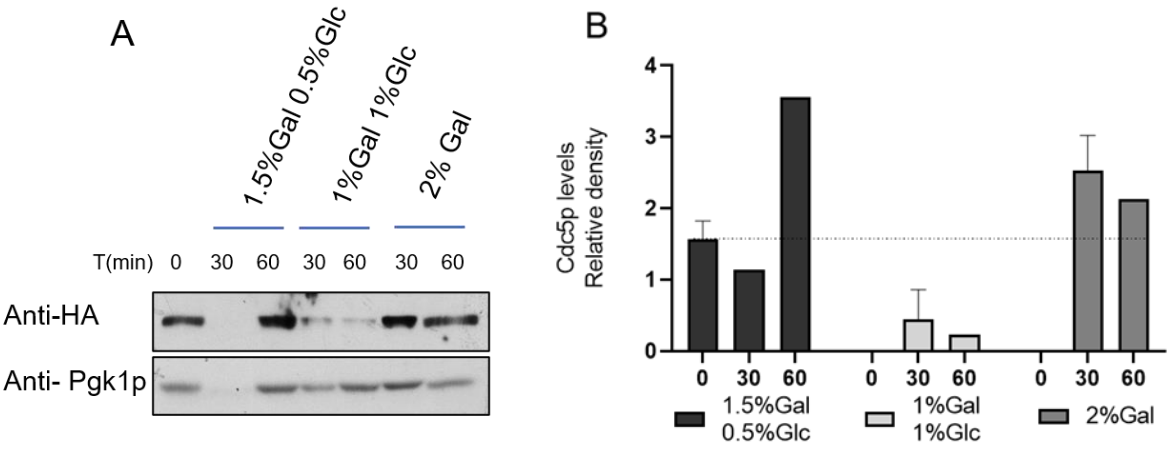

Figure 15 – Evaluation of Cdc5p expression under p*GAL1* regulation via western blot analysis. A. Analysis of Cdc5p expression, probed with anti-HA. Cells were collected after overnight growth in control conditions (t=0) and after incubation periods in control (1.5% Gal 0.5% Glc), repressing (1% Gal 1% Glc) and inducing (2% Gal) conditions (t=30 and t=60). Pgk1p, used as a loading control, is also shown. B. Graphical representation of Cdc5p levels, mean ± SD. Sample size is n=1 for t=60 and t=30 1.5% Gal 0.5% Glc and n=2 for the remaining conditions.

Protein expression increased after a 30-minute incubation period in inducing conditions. Protein repression is already effective at 30 minutes, so this was the time selected for the assays. These results confirm the expected simultaneous repressing and inducing capability of the promoter. No significant alterations in protein levels were detected in control cells between t=0 and t=30 samples (Figure 15B), indicating that cell collection and media exchange step does not seem to affect protein expression, since no other condition was altered, and therefore t=0 was used as the control condition.

To determine the effects of both conditions, repression and overexpression of Cdc5p, on the phosphorylation status of Atp2p, cell extracts were analyzed in Zn^{2+}Phos-Tag™ SDS-PAGE assays, as before, to confirm the previous results. In these assays, Atp2p phosphorylation in repression/overexpression conditions was evaluated by comparison with control cells (Figure 16B), and scores were attributed to each observed shift, as previously.

Results show that overexpression of Cdc5p causes a significant increase in the phosphorylation state of Atp2p, comparatively to the control condition (Figure 16C), which confirms the results obtained for p*MET25*-mediated Cdc5p overexpression. However, repressing Cdc5 expression does not decrease the phosphorylated state of Atp2p as expected, since less molecules of kinase would be available to phosphorylate Atp2p. This may indicate that 30 min of repression is not sufficient to observe effects in Cdc5 targets since dephosphorylation is a slower process than phosphorylation as it depends not only on kinase levels but also on the dephosphorylation by a phosphatase. Wild type cells were also grown in the same conditions and evaluated in Zn^{2+}Phos-Tag™ SDS-PAGE assays (Figure 16A). As observed in Figure 16C, inducing conditions seem to cause a slight increase in phosphorylation, comparatively to the control condition, which may be caused by the shift to a respiratory media.

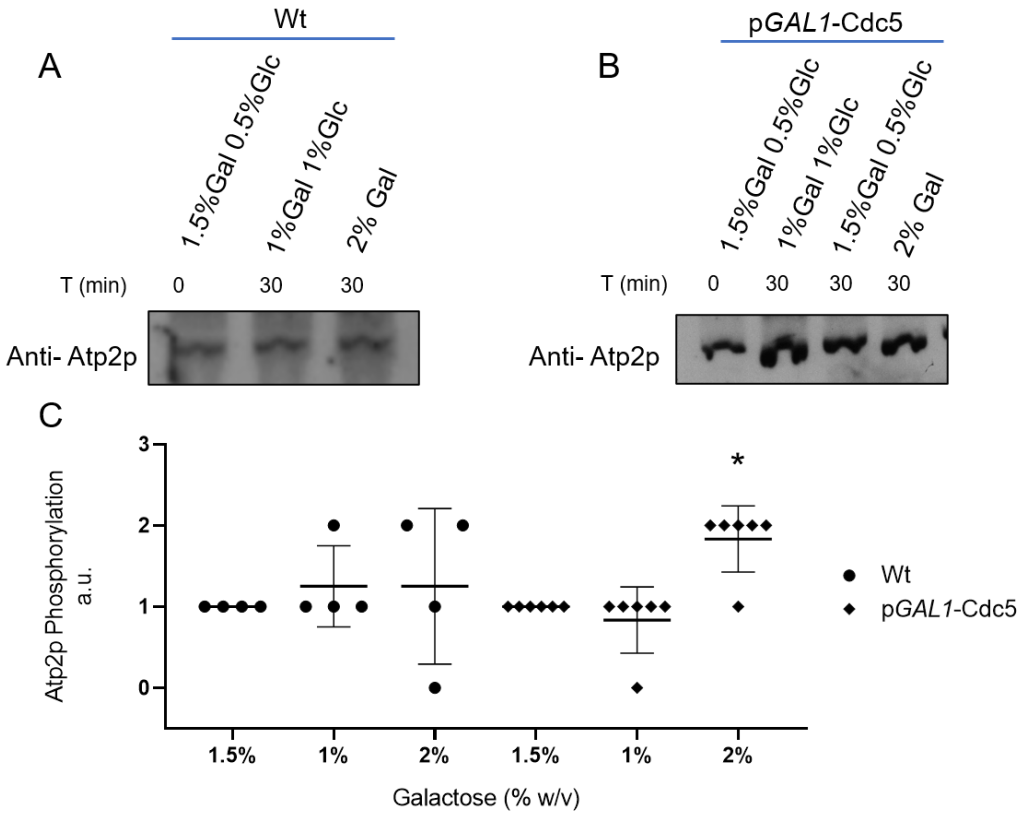

Figure 16 – Phos-Tag™ SDS-PAGE analysis of phosphorylation status of Atp2p for p*GAL1*-Cdc5 and wild type. A. Phosphorylation of Atp2p for wild type and (B) p*GAL1*-Cdc5 for whole cell extracts of control and both repressing and inducing conditions. C. Representation of the band shifts obtained for both repression and overexpression conditions of Wt and p*GAL1*-Cdc5. Each phosphorylation band was given a number according to its relative position compared its respective control (1.5%Gal 0.5%Glc). Each point represents a replica, mean ± SD is represented by each horizontal line and asterisk indicates significance ($p < 0.05$, Fisher's exact test against control – 1.5%Gal 0.5%Glc).

As before, Atp2p levels were also determined for both Cdc5 repressing and inducing conditions. Preliminary results (Figure 17) indicate a moderate but not significant increase in Atp2p levels in the repressed condition (1% Gal 1% Glc). This is in agreement with the lack of Atp2p dephosphorylation observed for these conditions (Figure 16C). For the inducing conditions there was also a small increase in Atp2p levels but a higher increase in Atp2 levels was estimated since the increase in Atp2 phosphorylation was evident. However, this may not be a representative result as the number of replicas is low.

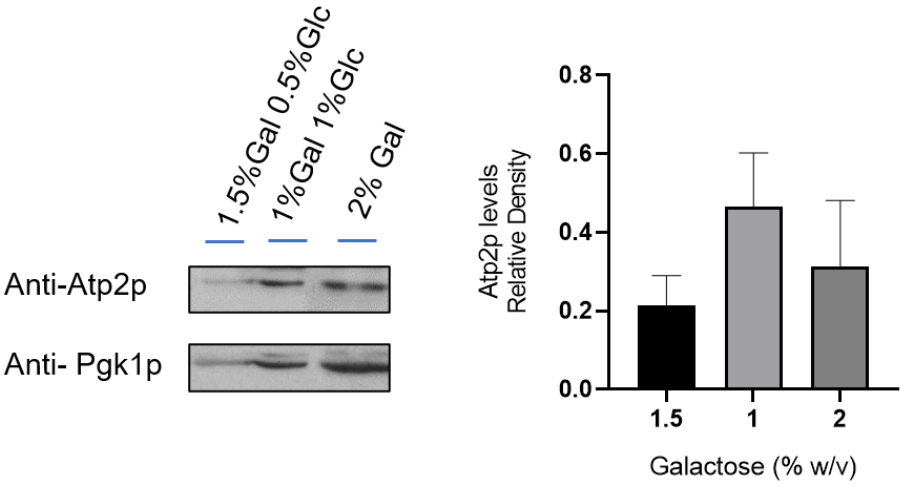

Figure 17 – Evaluation of Atp2p levels under p*GAL1* regulation. A. Analysis of Atp2p expression, probed with anti-atp2p. Cells were collected after overnight growth in control conditions (t=0) and after incubation periods in repressing (1% Gal 1% Glc) and inducing (2% Gal) conditions (t=30). Pgk1p, used as a loading control, is also shown. B. Semi-quantitative analysis of Atp2p levels for p*GAL1*-Cdc5, for control (1.5%Gal 0.5%Glc) as well as repressing (1%Gal 1%Glc) and inducing (2% Gal) conditions. Values are the mean ± SEM (n=2), one-way ANOVA, Tukey's test. No statistical significance between conditions.

3.4.1. Mitochondrial Respiration

As established previously, Atp2p is an essential component of the ATP synthase complex, which catalyzes the last reaction of the respiratory chain. It has also been described that increase in Atp2p phosphorylation ultimately leads to increased activity of the whole respiratory chain (Pereira *et al.*, 2018). Since our hypothesis is that overexpressing Cdc5p increases Atp2p phosphorylation, it is expected that it may lead to an increase in mitochondrial respiration.

To evaluate this, cells were grown in repressing, inducing and control conditions to test different levels of Cdc5p expression. Cells were grown until PDS and the oxygen consumption rate was measured using a Clark oxygen electrode. Results show that in inducing conditions, cells expressing p*GAL1-CDC5* present a clear increase in the respiratory rate, comparatively to the wild-type, in the same conditions, indicating that overexpressing Cdc5p does indeed increase respiratory function (Figure 18). Further work

will be required to evaluate whether this increase in respiration is dependent on Atp2p phosphorylation.

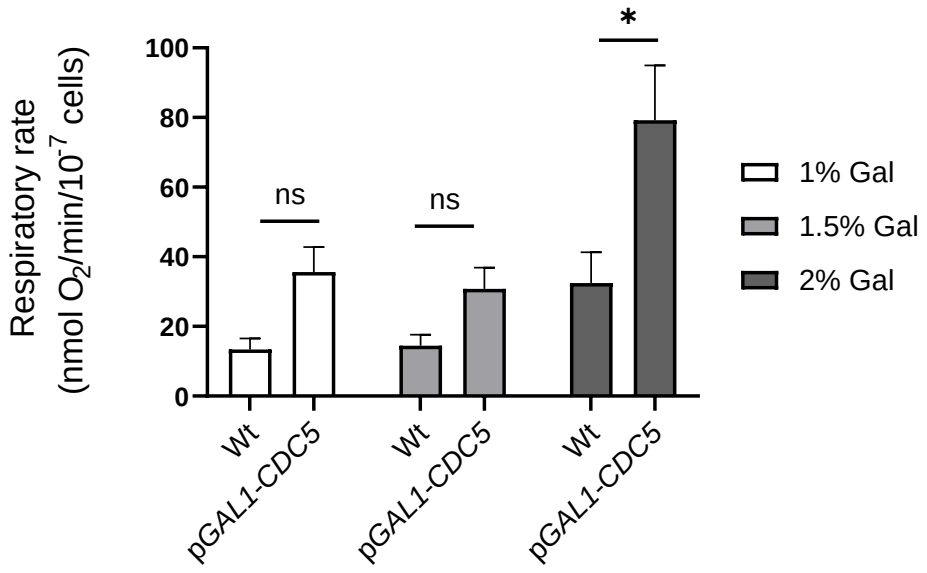

Figure 18 – Respiratory rate for p*GAL1*-Cdc5 and Wt. Values are mean ± SEM (n=4), two-way ANOVA, Tukey's test, *, $p < 0.05$.

3.4.2. Respiratory Growth

To confirm possible effects of Cdc5p on mitochondrial function, growth in respiratory media upon repression/overexpression of *CDC5* was evaluated. The remaining kinases were also tested. To do so, strains under regulation of the *MET25* promoter were plated on rich media containing glycerol, a strictly respiratory carbon source, in a ten-fold dilution series, as well as in YPD (fermentative media) which serves as control. In these rich media, methionine is abundant and kinases under regulation of p*MET25* should be repressed. Results show that strains with *IPL1*, *PKC1* and *HRR25* under *MET25* regulation, in the presence of methionine (Figure 19) exhibit normal growth when compared with the wt in both respiratory and fermentative media. Cdc28p (not shown) is also able to grow in both media. While we observed normal growth in fermentative media, Cdc5 is the only kinase unable to grow in respiratory media, suggesting that kinase expression is important for respiratory growth.

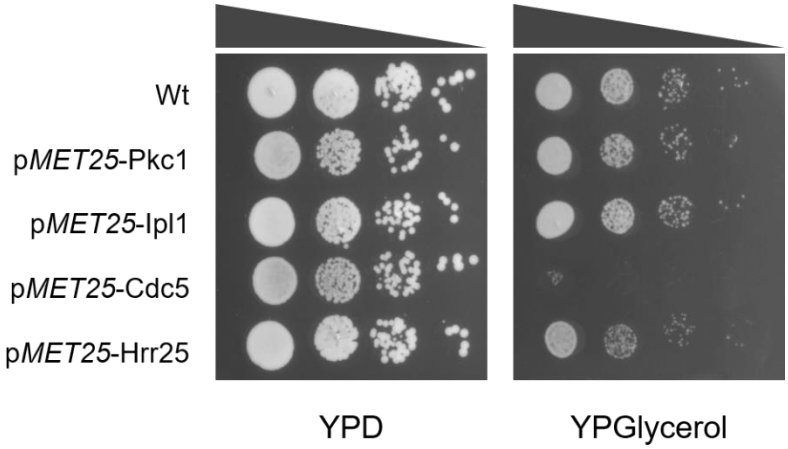

Figure 19 - Growth assessment in glycerol - strictly respiratory media and YPD – glucose-based media, used as control. Strains under regulation of p*MET25* and wt were spotted in a ten-fold dilution series (n=3).

3.4.3. *ATP2* and *CDC5*: Assessing a Possible Genetic Interaction

Discovery of genetic interactions not only sheds light on functional relations between genes but also helps elucidate the signaling pathway where those genes are integrated. To investigate a possible genetic interaction between *ATP2* and *CDC5*, new mutants were constructed to assess the effect of *ATP2* deletion in the growth defects caused by Cdc5p repression or overexpression.

Repression or overexpression of Cdc5p leads to growth defects due to cell cycle arrest (Walters 2014). In addition to the *ATP2* deletion, we also tested if the potential phosphorylation of Atp2p plays a role in the growth arrest caused by Cdc5p repression/overexpression. For that, Δ*atp2* p*GAL1*-Cdc5, expressing wt Atp2p [pRS316-*ATP2*] and the double phosphoresistant Atp2p mutant [pRS316-*ATP2*-Thr124A/Thr317A] were tested.

While in Cdc5p repressing conditions, we were not expecting differences between wt and phosphoresistant mutants, as in this case the Atp2 wt phosphorylation should be low, in overexpressing conditions, if the Atp2p phosphorylation is involved in growth defects mediated by Cdc5p, we should observe a growth improvement in cells expressing Atp2p-Thr124A/Thr317A phosphoresistant mutant.

The growth of these strains was then evaluated in solid media, with different sugar composition, to regulate Cdc5p expression via p*GAL1* regulation. Two Cdc5p repression

conditions were tested, 1% Gal 1% Glc and 2% Glc. As predicted, higher concentration of glucose led to poorer growth of strains expressing Cdc5p under regulation of the p*GAL1* (Figure 20). These results suggest that Atp2p or Atp2p phosphorylation do not have a role in the growth defects associated with Cdc5p repression. No growth inhibition was detected at 2% Gal, conditions in which Cdc5p should be overexpressed, and, therefore, we cannot conclude about the effect of Atp2p phosphorylation on growth defects associated with Cdc5 overexpression.

Concerning the *ATP2* null mutant, we did not detect a genetic interaction of *CDC5* with *ATP2* upon *CDC5* repression. This suggests that mediation of cell cycle arrest and Atp2 phosphoregulation by Cdc5 may be separate processes.

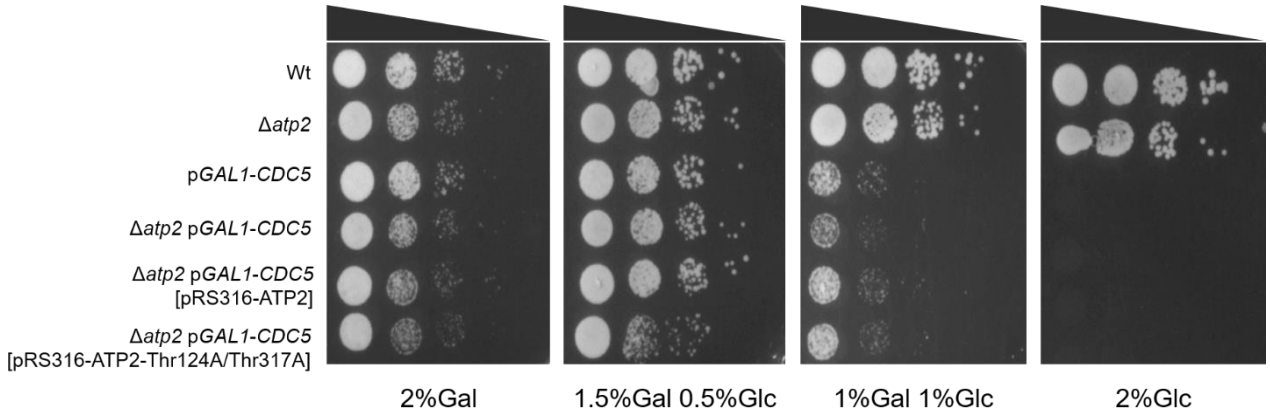

Figure 20 – Effect of different levels of Cdc5 expression, in the absence of Atp2p, in cell growth for various strains. Yeast cells were grown until PDS phase in YPC medium, then diluted to an OD_{600}=0.1 and four ten-fold dilution series were spotted on solid plates (n=3).

Since no phenotype was observed in solid media, the growth of the strains Δ*atp2* p*GAL1-CDC5* [pRS316-*ATP2*] and Δ*atp2* p*GAL1-CDC5* [pRS316-*ATP2*-Thr124A/Thr317A] was also evaluated in liquid media. We also tested, as a control, the growth of Δ*atp2* [pRS316-*ATP2*] and Δ*atp2* [pRS316-*ATP2*-Thr124A/Thr317A] in cells with wt Cdc5p (Figure 21A). Analysis of these growth curves, however, does not show any significant alteration in cellular growth, as observed from the calculated specific growth rate (Figure 21B).

Yet, and similarly to the growth in solid media, growth inhibition caused by Cdc5p overexpression was negligible, which is unexpected as overexpression of Cdc5p is linked with growth defects caused by cell cycle arrest (Kitada *et al.*, 1993; Walters *et al.*, 2014). In

the absence of a *CDC5*-overexpression phenotype, it is not possible to conclude on the role of Atp2p phosphorylation on *CDC5*-induced growth arrest.

A

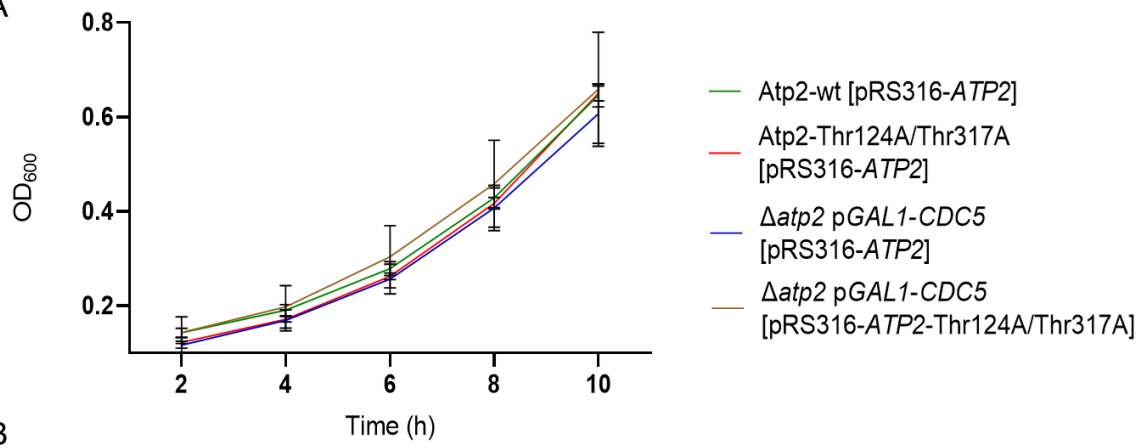

B

Strain	Specific Growth Rate
Atp2-wt [pRS316-*ATP2*]	**0.76 ± 0.03**
Atp2-Thr124A/Thr317A [pRS316-*ATP2*]	**0.79 ± 0.03**
Δ*atp2* p*GAL1-CDC5* [pRS316-*ATP2*]	**0.73 ± 0.10**
Δ*atp2* p*GAL1-CDC5* [pRS316-*ATP2*-Thr124A/Thr317A]	**0.77 ± 0.18**

Figure 21 - Analysis of cell growth. A. Cells of the strains Atp2-wt [pRS316-*ATP2*], Atp2-Thr124A/Thr317A [pRS316-*ATP2*], Δ*atp2* p*GAL1-CDC5* [pRS316-*ATP2*] and Δ*atp2* p*GAL1-CDC5* [pRS316-*ATP2*-Thr124A/Thr317A] were inoculated in inducing conditions and their respective growth was monitored by OD_{600} measurements over a period of 10 hours. Values are mean ± SD (n=3), Two-way ANOVA, Tukey's test. None of the strains reached statistical significance. B. Specific growth rate for the previous strains. Values are mean ± SD (n=3).

4. Final Considerations

ATP synthase is a mitochondrial protein complex, highly conserved from yeast to humans, responsible for the production of the majority of cellular ATP. Dysregulation of its activity has been associated with human diseases such as diabetes and numerous cardiac disorders. In yeast, the β subunit of ATP synthase has been shown to be regulated by post-translational modifications such as phosphorylation. Pereira *et al*. identified two phosphorylated residues, Thr124 and Thr317, in *Saccharomyces cerevisiae's* β subunit, that are targeted by Sit4p (Pereira *et al.*, 2018). However, the kinases that regulate these phosphosites remain unknown, and its identification was the main goal of the present study.

Using an *in silico* prediction software, based on motif recognition, 4 kinases were predicted to regulate Atp2p. All selected kinases, Ipl1, Pkc1, Hrr25, Cdc5, have known roles in cell cycle events. In addition, the phosphatase identified as a regulator of these residues, Sit4p, also plays important roles in cell cycle progression, namely regulation of G1 cyclin genes (Pereira *et al.*, 2018). Taking this into account, it is possible that phosphorylation of Thr124 and Thr317 may be regulated during cell cycle and play a role in this process.

The kinases predicted *in silico* are all encoded by essential genes, and therefore, gene deletion is not a viable option for their study. We opted for the use of an inducible promoter, p*MET25*. However, as discussed before, this promoter is not efficiently repressed so, in non-inducing/repressing conditions, we cannot be certain that kinase levels are actually decreasing. In fact, looking specifically at Cdc5, since its repression by glucose (under the control of p*GAL1*) leads to decreased growth in solid media, and the same is not observed for cells under the control of p*MET25* in the presence of methionine, we may speculate that even in repressing conditions we may have more expression than under the regulation of the endogenous promoter. This would be in agreement with the results obtained for the Atp2p phosphorylation in the putative repressing conditions, in which an increase in phosphorylation was observed instead of a decrease. To clarify this issue, it will be important to tag each kinase in the wild type with a C-terminal tag to allow detection and quantification of protein levels, since no specific antibody for each kinase is commercially available, which can then be compared with the protein levels obtained for p*MET25*-mediated repression.

In general, the 4 predicted kinases seem to influence Atp2p phosphorylation, when kinase expression is manipulated. This is not the case for Cdc28, the only evaluated kinase

that was not predicted using bioinformatics tools, which supports the robustness of the *in silico* predictions. In fact, Pkc1p is the only protein kinase C in *S. cerevisiae*, homolog to the mammalian isozymes of PKC that have been suggested as regulators of several ATP synthase subunits, including β (A. Johnson and Ogbi, 2011; Dave *et al.*, 2011). Additionally, Pkc1 has been reported to share substrates with the phosphatase Sit4p, which regulates Atp2p, making this kinase an interesting candidate.

Since expression of Hrr25p could not be effectively regulated under the *MET25* promoter and the two other alternatives pursued were also unsuccessful, the effects of this kinase on Atp2 phosphorylation could not be evaluated. Nevertheless, under regulation of p*MET25*, Hrr25p caused Atp2p phosphorylation and as it shares substrates with Sit4p, it may also be a promising candidate to be an Atp2 regulator.

The most promising kinase from the Phos-Tag™ assays was Cdc5 since its overexpression resulted in increased phosphorylation of Atp2p, under regulation of p*MET25*. These results were consistent with overexpression under regulation of p*GAL1*. Since this kinase was selected based on the sequence that integrates one of the phosphosites of interest, Thr124, we can assume that alterations in the phosphorylation status of Atp2 are reflective of phosphoregulation of this residue.

Overexpression of Cdc5p resulted in significant increase in the respiratory rate, comparatively to the wild type, which suggests increased respiratory function. This is supported by the inability of p*MET25*-Cdc5 to grow in rich strictly respiratory media, indicating an important role of Cdc5 in respiratory function.

Cdc5p has been described as necessary for mitochondria segregation and consequent transmission of mtDNA (Dutcher, 1982) but, to our knowledge, no role in the regulation of mitochondrial respiration was described so far. The increase in respiratory rate observed in this study constitutes, therefore, a novel, previously unsuspected role for Cdc5, which needs further characterization.

CDC5 repression resulted in growth inhibition in glycerol, a strictly respiratory media, which may be justified by loss of mtDNA, whose transmission depends on Cdc5p expression. The endogenous Atp2p levels upon *CDC5* repression with either p*MET25* or p*GAL1*, are overall much lower than for the remaining kinases, which could also be explained by loss of mitochondrial DNA, as discussed before.

Overall, these results suggest an interaction between Cdc5p and Atp2p, since overexpression of Cdc5p causes increased phosphorylation of Atp2p and increased protein levels, as well as increased respiratory function. However, this information is not sufficient to conclude if Cdc5p is a phosphoregulator of Atp2p. To ascertain if increased respiratory rate is a result of increased Atp2p phosphorylation, the respiratory rate of Cdc5 overexpression in the absence of Atp2 phosphorylation (expressing the Atp2p phosphoresistant double mutant), should also be evaluated. If this is the case, respiratory rate should decrease upon expression of the double phosphoresistant mutant since phosphorylation of Thr124/Thr317 is blocked. Therefore, this assay is important to determine if Atp2p is involved in the increased mitochondrial function upon Cdc5 overexpression.

Additionally, to confirm if Cdc5p phosphoregulates Atp2, co-immunoprecipitation and *in vitro* kinase assays should be performed. Co-immunoprecipitation assays should clarify if Cdc5p and Atp2p have a physical interaction, since this technique allows isolation and precipitation of protein complexes, in this case Atp2p-Cdc5p. Finally, *in vitro* kinase assays should also be performed to verify if Cdc5p is actively phosphorylating Atp2p, to demonstrate that the effect on Atp2p phosphorylation is directly caused by Cdc5p and not by an intermediary involved in this signaling pathway.

In recent years, many phosphorylation sites have been described in all subunits of ATP synthase, including the β subunit. Nonetheless, the majority of modified residues remain unidentified and the kinases responsible for the regulation of these phosphosites are also unknown. Identifying regulatory kinases of the β subunit of ATP synthase could be important in our understanding of how this enzymatic complex is regulated, particularly because the residues are conserved in mammals and can affect overall mitochondrial respiration. In the long run, a deeper understanding of the regulating mechanisms of ATP synthase as well as understanding the functional consequences of these modifications in pathological conditions may be useful in development of therapeutics and pharmaceutical drugs for treatment of human diseases, such as diabetes and stroke.

5. References

A. Johnson, J. and Ogbi, M. (2011) ‘Targeting the F1Fo ATP Synthase: Modulation of the Bodys Powerhouse and Its Implications for Human Disease‘, *Current Medicinal Chemistry*, 18(30), pp. 4684-4714. doi: 10.2174/092986711797379177.

Ackerman, S. H. and Tzagoloff, A. (2005) ‘Function, Structure, and Biogenesis of Mitochondrial ATP Synthase‘, *Progress in Nucleic Acid Research and Molecular Biology*, 80(November), pp. 95–133. doi: 10.1016/S0079-6603(05)80003-0.

Agnetti, G. *et al.* (2007) ‘Proteomic technologies in the study of kinases: Novel tools for the investigation of PKC in the heart’, *Pharmacological Research*, 55(6), pp. 511–522. doi: 10.1016/j.phrs.2007.04.012.

Alberts, B. *et al.* (2013) *Essential Cell Biology*. 4th edn., pp. 447-458, W. W. Norton & Company.

Arrell, D. K. *et al.* (2006) ‘Proteomic analysis of pharmacological preconditioning: Novel protein targets converge to mitochondrial metabolism pathways’, *Circulation Research*, 99(7), pp. 706–714. doi: 10.1161/01.RES.0000243995.74395.f8.

Biner, O. *et al.* (2018) ‘Towards a synthetic mitochondrion’, *Chimia*, 72(5), pp. 291–296. doi: 10.2533/chimia.2018.291.

Buvelot, S. *et al.* (2003) ‘The budding yeast Ipl1/Aurora protein kinase regulates mitotic spindle disassembly’, *Journal of Cell Biology*, 160(3), pp. 329–339. doi: 10.1083/jcb.200209018.

Cabezón, E. *et al.* (2000) ‘Dimerization of bovine F1-ATPase by binding the inhibitor protein, IF1’, *Journal of Biological Chemistry*, 275(37), pp. 28353–28355. doi: 10.1074/jbc.C000427200.

Carraro, M. *et al.* (2014) ‘Channel formation by yeast F-ATP synthase and the role of dimerization in the mitochondrial permeability transition’, *Journal of Biological Chemistry*, 289(23), pp. 15980–15985. doi: 10.1074/jbc.C114.559633.

Castellanos, E. and Lanning, N. J. (2019) ‘Phosphorylation of OXPHOS machinery subunits: Functional implications in cell biology and disease’, *Yale Journal of Biology and Medicine*, 92(3), pp. 523–531.

Cheng, H.-C. *et al.* (2011) ‘Regulation and function of protein kinases and phosphatases’, *Enzyme Research*, 2011(1), pp. 7–10. doi: 10.4061/2011/794089.

Covian, R. and Balaban, R. S. (2012) ‘Cardiac mitochondrial matrix and respiratory complex protein phosphorylation’, *American Journal of Physiology - Heart and Circulatory Physiology*, 303(8), pp. 940–966. doi: 10.1152/ajpheart.00077.2012.

Dautant, A. *et al.* (2018) ‘ATP Synthase Diseases Of Mitochondrial Genetic Origin’, *Frontiers in Physiology*, 9(329), pp. 1–16. doi: 10.3389/fphys.2018.00329.

Dave, K. R. *et al.* (2011) ‘Activation of Protein Kinase C Delta following Cerebral Ischemia Leads to Release of Cytochrome C from the Mitochondria via Bad Pathway’, *PLoS ONE*, 6(7), pp. 1–9. doi: 10.1371/journal.pone.0022057.

Davies, K. M. *et al.* (2012) ‘Structure of the yeast F 1F o-ATP synthase dimer and its role in shaping the mitochondrial cristae’, *Proceedings of the National Academy of Sciences of the United States of America*, 109(34), pp. 13602–13607. doi: 10.1073/pnas.1204593109.

Detmer, S. A. and Chan, D. C. (2007) ‘Functions and dysfunctions of mitochondrial dynamics’, *Nature Reviews Molecular Cell Biology*, 8(11), pp. 870–879. doi: 10.1038/nrm2275.

Dohmen, R. J., Wu, P. and Varshavsky, A. (1994) ‘Heat-Inducible Degron : A Method for Constructing Temperature-Sensitive Mutants’, 263(March), pp. 1273–1276. doi: 10.1126/science.8122109.

Dutcher, S. K. (1982) ‘Two cell division cycle mutants of Saccharomyces cerevisiae are defective in transmission of mitochondria to zygotes’, *Genetics*, 102(1), pp. 9–17.

Faccenda, D. and Campanella, M. (2012) ‘Molecular regulation of the mitochondrial F1F o-ATPsynthase: Physiological and pathological significance of the Inhibitory Factor 1 (IF1)’, *International Journal of Cell Biology*, 2012, pp. 1–12. doi: 10.1155/2012/367934.

Filograna, R. *et al.* (2020) ‘Mitochondrial DNA copy number in human disease: the more the better?’, *FEBS Letters*, 2020, pp. 1–27. doi: 10.1002/1873-3468.14021.

Foury, F. (1997) ‘Human genetic diseases : a cross-talk between man and yeast’, *Gene*, 195, pp. 1–10. doi: 10.1016/s0378-1119(97)00140-6.

Frankovsky, J. *et al.* (2021) ‘Mitochondrion protein phosphorylation in yeast revisited’, *Mitochondrion*, 57(October 2020), pp. 148–162. doi: 10.1016/j.mito.2020.12.016.

Frey, T. G. and Mannella, C. A. (2000) ‘The internal structure of mitochondria’, *Trends in Biochemical Sciences*, 0004(July), pp. 319–324. doi: 10.1016/s0968-0004(00)01609-1.

García-Rodríguez, L. J. *et al.* (2009) ‘Mitochondrial Inheritance Is Required for MEN-Regulated Cytokinesis in Budding Yeast’, *Current Biology*, 19(20), pp. 1730–1735. doi:

10.1016/j.cub.2009.08.041.

Gietz, R. D. and Schiestl, R. H. (2007) 'High-efficiency yeast transformation using the LiAc/SS carrier DNA/PEG method', *Nature Protocols*, 2(1), pp. 31–34. doi: 10.1038/nprot.2007.13.

Giorgio, V. *et al.* (2013) 'Dimers of mitochondrial ATP synthase form the permeability transition pore', *Proceedings of the National Academy of Sciences of the United States of America*, 110(15), pp. 5887–5892. doi: 10.1073/pnas.1217823110.

Hermann, G. J. and Shaw, J. M. (1998) 'Mitochondrial Dynamics in Yeast', *Annual Review of Cell and Developmental Biology*, 14(1), pp. 265–303. doi: 10.1146/annurev.cellbio.14.1.265.

Højlund, K. *et al.* (2009) 'Human ATP synthase beta is phosphorylated at multiple sites and shows abnormal phosphorylation at specific sites in insulin-resistant muscle', *Diabetologia*, 53(3), pp. 541–551. doi: 10.1007/s00125-009-1624-0.

Hopper, R. K. *et al.* (2006) 'MITOCHONDRIA MATRIX PHOSPHOPROTEOME: EFFECT OF EXTRA MITOCHONDRIAL CALCIUM', *Biochemistry*, 45(8), pp. 2524–2536. doi: 10.1021/bi052475e.

Huttlin, E. L. *et al.* (2010) 'A Tissue-Specific Atlas of Mouse Protein Phosphorylation and Expression', *Cell*, 143(7), pp. 1174–1189. doi: 10.1016/j.cell.2010.12.001.

Janke, C. *et al.* (2004) 'A versatile toolbox for PCR-based tagging of yeast genes: new fluorescent proteins, more markers and promoter substitution cassettes', *Yeast*, 21(11), pp. 947–962. doi: 10.1002/yea.1142.

Kafadar, K. A. *et al.* (2003) 'Negative regulation of calcineurin signaling by Hrr25p, a yeast homolog of casein kinase I', *Genes and Development*, 17(21), pp. 2698–2708. doi: 10.1101/gad.1140603.

Kane, L. A. *et al.* (2010) 'Phosphorylation of the F1Fo ATP synthase β subunit: Functional and structural consequences assessed in a model system', *Circulation Research*, 106(3), pp. 504–513. doi: 10.1161/CIRCRESAHA.109.214155.

Kane, L. A. and Van Eyk, J. E. (2009) 'Post-translational modifications of ATP synthase in the heart: biology and function', *Journal of Bioenergetics and Biomembranes*, 41(2), pp. 145–150. doi: 10.1007/s10863-009-9218-6.Post-translational.

Kanekatsu, M. *et al.* (1998) 'THE BETA SUBUNIT OF CHLOROPLAST ATP SYNTHASE (CFoCF1-ATPase) IS PHOSPHORYLATED BY CASEIN KINASE II',

Biochemistry and Molecular Biology International, 46(1), pp. 99–105. doi: 10.1080/15216549800203602.

Kanfer, G. and Kornmann, B. (2016) 'Dynamics of the mitochondrial network during mitosis', *Biochemical Society Transactions*, 44(2), pp. 510–516. doi: 10.1042/BST20150274.

Karathia, H. *et al.* (2011) 'Saccharomyces cerevisiae as a Model Organism: A Comparative Study', *PLoS ONE*. Edited by G. de Polavieja, 6(2), pp. 1–10. doi: 10.1371/journal.pone.0016015.

Karp, G., Iwasa, J. and Marshall, W. (2015) *Karp's Cell and Molecular Biology: Concepts and Experiments*. 8th edn. pp. 168-198, Wiley.

Kinoshita, E. and Kinoshita-Kikuta, E. (2011) 'Improved Phos-tag SDS-PAGE under neutral pH conditions for advanced protein phosphorylation profiling', *Proteomics*, 11(2), pp. 319–323. doi: 10.1002/pmic.201000472.

Kitada, K. *et al.* (1993) 'A multicopy suppressor gene of the Saccharomyces cerevisiae G1 cell cycle mutant gene dbf4 encodes a protein kinase and is identified as CDC5.', *Molecular and Cellular Biology*, 13(7), pp. 4445–4457. doi: 10.1128/MCB.13.7.4445.

Koopmman, W. J. H., Willems, P. H. G. . and Smeitink, J. A. M. (2012) 'Monogenic Mitochondrial Disorders', *The new england journal of medicine*, 366(12), pp. 1132–1141. doi: 10.1056/NEJMra1012478.

De La Torre-Ruiz, M. A. *et al.* (2002) 'Sit4 is required for proper modulation of the biological functions mediated by Pkc1 and the cell integrity pathway in Saccharomyces cerevisiae', *Journal of Biological Chemistry*, 277(36), pp. 33468–33476. doi: 10.1074/jbc.M203515200.

Larsson, N. and Clayton, D. A. (1995) 'MOLECULAR GENETIC ASPECTS OF HUMAN MITOCHONDRIAL DISORDERS', *Annual Review of Genetics*, 29, pp. 151–178. doi: 10.1146/annurev.ge.29.120195.001055.

Lasserre, J.-P. *et al.* (2015) 'Yeast as a system for modeling mitochondrial disease mechanisms and discovering therapies', *Disease Models and Mechanisms*, 8(6), pp. 509–526. doi: 10.1242/dmm.020438.

Lee, J. *et al.* (2007) 'Mitochondrial Phosphoproteome Revealed by an Improved IMAC Method and MS/MS/MS', *Molecular and Cellular Proteomics*, 6(4), pp. 669–676. doi: 10.1074/mcp.M600218-MCP200.

Long, Q., Yang, K. and Yang, Q. (2015) ‘Regulation of mitochondrial ATP synthase in cardiac pathophysiology’, *American Journal of Cardiovascular Disease*, 5(1), pp. 19–32.

Malina, C., Larsson, C. and Nielsen, J. (2018) ‘Yeast mitochondria: An overview of mitochondrial biology and the potential of mitochondrial systems biology’, *FEMS Yeast Research*, 18(5), pp. 1–17. doi: 10.1093/femsyr/foy040.

McDonald, M., Trost, B. and Napper, S. (2018) ‘Conservation of kinase-phosphorylation site pairings: Evidence for an evolutionarily dynamic phosphoproteome’, *PLoS ONE*, 13(8), pp. 1–11. doi: 10.1371/journal.pone.0202036.

Mehlgarten, C. *et al.* (2009) ‘Elongator function depends on antagonistic regulation by casein kinase Hrr25 and protein phosphatase Sit4’, *Molecular Microbiology*, 73(5), pp. 869–881. doi: 10.1111/j.1365-2958.2009.06811.x.

Mendenhall, M. D. and Hodge, A. E. (1998) ‘Regulation of Cdc28 cyclin-dependent protein kinase activity during the cell cycle of the yeast Saccharomyces cerevisiae.’, *Microbiology and molecular biology reviews*, 62(4), pp. 1191–1243.

Nelson, D. L., Lehninger, A. L. and Cox, M. M. (2008) *Lehninger Principles of Biochemistry*. 5th edn. pp. 723-731, Macmillan.

Nguyen, T., Ogbi, M. and Johnson, J. A. (2008) ‘Delta protein kinase C interacts with the d subunit of the F1Fo ATPase in neonatal cardiac myocytes exposed to hypoxia or phorbol ester: Implications for F1Fo ATPase regulation’, *Journal of Biological Chemistry*, 283(44), pp. 29831–29840. doi: 10.1074/jbc.M801642200.

Nowak, G. and Bakajsova, D. (2015) ‘Protein kinase C-α interaction with FoF1-ATPase promotes FoF1-ATPase activity and reduces energy deficits in injured renal cells’, *Journal of Biological Chemistry*, 290(11), pp. 7054–7066. doi: 10.1074/jbc.M114.588244.

Ohlmeier, S., Hiltunen, J. K. and Bergmann, U. (2010) ‘Protein phosphorylation in mitochondria - A study on fermentative and respiratory growth of Saccharomyces cerevisiae’, *Electrophoresis*, 31(17), pp. 2869–2881. doi: 10.1002/elps.200900759.

Paumard, P. *et al.* (2002) ‘The ATP synthase is involved in generating mitochondrial cristae morphology’, *The EMBO Journal*, 21(3), pp. 221–230. doi: 10.1093/emboj/21.3.221.

Pereira, C. *et al.* (2018) ‘Sit4p-mediated dephosphorylation of Atp2p regulates ATP synthase activity and mitochondrial function’, *Biochimica et Biophysica Acta (BBA) - Bioenergetics*. Elsevier, 1859(8), pp. 591–601. doi: 10.1016/j.bbabio.2018.04.011.

Rampelt, H. *et al.* (2017) ‘Role of the mitochondrial contact site and cristae organizing

system in membrane architecture and dynamics', *Biochimica et Biophysica Acta - Molecular Cell Research*. Elsevier B.V., 1864(4), pp. 737–746. doi: 10.1016/j.bbamcr.2016.05.020.

Reiland, S. *et al.* (2009) 'Large-scale arabidopsis phosphoproteome profiling reveals novel chloroplast kinase substrates and phosphorylation networks', *Plant Physiology*, 150(2), pp. 889–903. doi: 10.1104/pp.109.138677.

Reinders, J. *et al.* (2007) 'Profiling phosphoproteins of yeast mitochondria reveals a role of phosphorylation in assembly of the ATP synthase', *Molecular and Cellular Proteomics*, 6(11), pp. 1896–1906. doi: 10.1074/mcp.M700098-MCP200.

Scorrano, L. *et al.* (2002) 'A distinct pathway remodels mitochondrial cristae and mobilizes cytochrome c during apoptosis', *Developmental Cell*, 2(1), pp. 55–67. doi: 10.1016/S1534-5807(01)00116-2.

Sierra, H. *et al.* (2015) 'Confocal Imaging–Guided Laser Ablation of Basal Cell Carcinomas: An Ex Vivo Study', *Journal of Investigative Dermatology*, 135(2), pp. 612–615. doi: 10.1016/s0962-8924(01)02246-2.

Simpson-Lavy, K. J. and Brandeis, M. (2011) 'Phosphorylation of Cdc5 regulates its accumulation', *Cell Division*, 6(23), pp. 1–6. doi: 10.1186/1747-1028-6-23.

Stock, D. *et al.* (2000) 'The rotary mechanism of ATP synthase', *Current Opinion in Structural Biology*, 10(6), pp. 672–679. doi: 10.1016/S0959-440X(00)00147-0.

Wako (2016) 'Phos-tag SDS-PAGE GUIDEBOOK', pp. 1–31. Available at: https://labchem-wako-pages.fujifilm.com/US-Phostag-Catalog-Download.html.

Wallace, D. C., Brown, M. D. and Lott, M. T. (1999) 'Mitochondrial DNA variation in human evolution and disease', *Gene*, 238, pp. 211–230. doi: 10.1016/s0378-1119(99)00295-4.

Walters, A. D. *et al.* (2014) 'The yeast polo kinase Cdc5 regulates the shape of the mitotic nucleus', *Current Biology*. Elsevier Ltd, 24(23), pp. 2861–2867. doi: 10.1016/j.cub.2014.10.029.

Westermann, B. (2012) 'Bioenergetic role of mitochondrial fusion and fission', *Biochimica et Biophysica Acta - Bioenergetics*. Elsevier B.V., 1817(10), pp. 1833–1838. doi: 10.1016/j.bbabio.2012.02.033.

Willers, I. M. and Cuezva, J. M. (2011) 'Post-transcriptional regulation of the mitochondrial H+-ATP synthase: A key regulator of the metabolic phenotype in cancer', *Biochimica et Biophysica Acta - Bioenergetics*. Elsevier B.V., 1807(6), pp. 543–551. doi:

10.1016/j.bbabio.2010.10.016.

Xue, Y. *et al.* (2008) 'GPS 2.0, a tool to predict kinase-specific phosphorylation sites in hierarchy', *Molecular and Cellular Proteomics*, 7(9), pp. 1598–1606. doi: 10.1074/mcp.M700574-MCP200.

Zhao, X. *et al.* (2011) 'Phosphoproteome analysis of functional mitochondria isolated from resting human muscle reveals extensive phosphorylation of inner membrane protein complexes and enzymes', *Molecular and Cellular Proteomics*, 10(1), pp. 1–14. doi: 10.1074/mcp.M110.000299.

6. Supplementary Figures

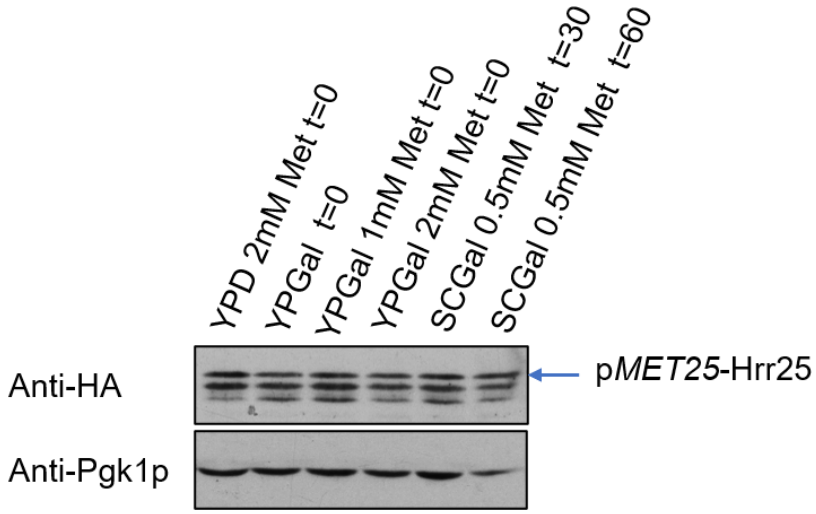

Figure S1 – Western Blot analysis of p*MET25*-Hrr25, probed with anti-HA, to evaluate protein expression. Cells were grown overnight in four different media: YPD 2mM Met; YPGal; YPGal 1mM Met; YPGal 2mM Met. Cells grown in YPGal 2mM Met were washed, inoculated in SCGal 0.5mM Met and collected after 30 and 60 minutes. A loading control, Pgk1p, is also shown.

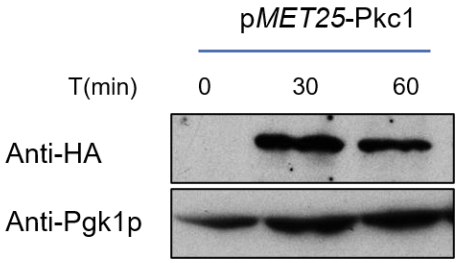

Figure S2 – Western Blot analysis of p*MET25*-Pkc1, probed with anti-HA, to evaluate protein expression. Cells were collected after overnight growth in repressing conditions (t=0) and two time points, 30 and 60 minutes, were collected after incubation in inducing conditions. A loading control, Pgk1p, is also shown.

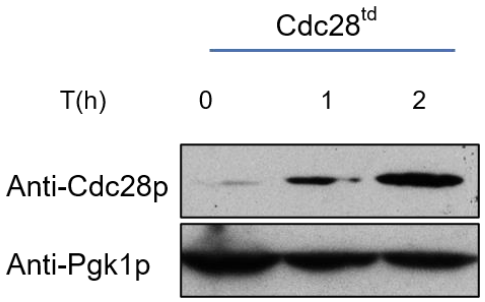

Figure S3 - Western Blot analysis of $Cdc28^{td}$, probed with anti-Cdc28p, to evaluate protein expression. Cells were collected after growth at the restrictive temperature for 3h (t=0) and two time-points, 1 and 2 hours, were collected after incubation at the permissive temperature. A loading control, Pgk1, is also shown.